Multiparametric cardiovascular magnetic resonance characterisation of myocardial inflammation in patients with rheumatic heart disease

by

PETRONELLA SAMUELS

Thesis submitted in fulfilment of the requirements for the degree

Master of Science in Radiography

in the Faculty of Health and Wellness Sciences

at the Cape Peninsula University of Technology

Supervisor: Mr A. Speelman
Co-supervisors: Professor N.A.B. Ntusi & Mrs E. Herbert

Bellville
October 2020

DEDICATION

“Trust in the Lord with all your heart and lean not on your own understanding”
Proverbs 3:5-6

To my husband, Lionel, for your unconditional love and support. My precious daughters, Jade, Robyn and Reese, and my grandson Damon, for helping me believe in myself.

To my late mother, who, despite hardships, always gave her best. You were undoubtedly one of the most resilient women I have ever known.

“Challenges are what make life interesting and overcoming them is what makes life meaningful”

Joshua J. Marine

ACKNOWLEDGEMENTS

I wish to thank:

- Aladdin Speelman, my academic supervisor, for his guidance, support and willingness to assist with everything. I appreciate your continued encouragement.
- Estelle Herbert, my academic co-supervisor, for her support and kind words of encouragement.
- Professor Ntobeko Ntusi, my clinical co-supervisor and mentor, for affording me this opportunity to enrich myself, for believing in me and in doing so, helping me to better myself. I appreciate your continued support immensely.
- Dr Sarah Kraus, my collaborator, for taking time out of her busy schedule to share her knowledge and expertise and to guide me during this process. Your inspiration made it easy to complete this challenging task.
- Aremu O. Olukayode, recruiter and co-investigator on the study. You were a great pillar of strength during this challenging journey.
- Stephen Jermy, for assisting with the post-processing of the data.
- Dr. C. Uys for sharing her expertise and assisting me with the statistical analysis.
- Patricia Maishi, Ingrid Opt'Hoff and Mariaan Jaftha for their assistance with scanning of the patients and controls.
- Dr Marcin Jankiewicz for his assistance and guidance.
- Professor Ernesta Meintjes and Daniel Doetz for their support.
- My husband, Lionel and girls, Jade, Robyn and Reese and my grandson, Damon, for their unconditional love and support, and for believing in me.

- My family and friends for their kind words of encouragement.
- The National Research Foundation for providing the funding for research.
- The late Professor Bongani Mayosi for the pivotal role that he played in bringing CMR to the African continent.

DECLARATION

I, **Petronella Samuels**, declare that the contents of this dissertation/thesis represent my own unaided work, and that the dissertation/thesis has not previously been submitted for academic examination towards any qualification. Furthermore, it represents my own opinions and not necessarily those of the Cape Peninsula University of Technology.

11 October 2020

Signed **Date**

PLAGIARISM DECLARATION

I, **Petronella Samuels**, confirm that this thesis is my own work and is not copied from any other person's work (published or unpublished).

11 October 2020

_____ _____

Signed **Date**

TABLE OF CONTENTS

LIST OF TABLES

LIST OF FIGURES

APPENDICES

ABBREVIATIONS

3D	Three dimensional
3T	Three Tesla
AF	Atrial fibrillation
AHA	American Heart Association
AR	Aortic regurgitation
ARF	Acute rheumatic fever
AS	Aortic stenosis
ASOT	Anti-streptolysin O titer
AV	Aortic valve
BMI	Body mass index
BPM	Beats per minute
BSA	Body surface area
BW	Bandwidth
CI	Confidence interval
CMR	Cardiovascular magnetic resonance
COR	Coronal
CPUT	Cape Peninsula University of Technology
CRMR	Chronic rheumatic mitral regurgitation
CRP	C-reactive protein
CVI	Circle cardiovascular imaging
DNase	Deoxyribonuclease
EDV	End diastolic volume
ECV	Extracellular volume
ECG	Electrocardiographic gating

ECM	Extracellular matrix
ECV	Extracellular volume
EF	Ejection fraction
eGFR	Estimated glomerular filtration rate
ESR	Erythrocyte sedimentation rate
ESV	End-systolic volume
FA	Flip angle
GAS	Group A Streptococcus
GBCA	Gadolinium based contrast agent
HASTE	Half-Fourier-Acquired Single-shot Turbo Spin Echo
He	Helium
HIV	Human immunodeficiency virus
HPCSA	Health Professions Council of South Africa
IFN	Interferon
IL	Interleukin
IR	Inversion recovery
kg	Kilograms
LGE	Late gadolinium enhancement
LL	Look-Locker
LMICs	Low- and middle-income countries
LV	Left ventricle/left ventricular
LVMi	Left ventricular mass indexed
LVEDV	Left ventricular end-diastolic volume
LVEDVi	Left ventricular end-diastolic volume indexed
LVEF	Left ventricular ejection fraction

LVESV	Left ventricular end-systolic volume
LVESVi	Left ventricular end-systolic volume indexed
LVOT	Left ventricular outflow tract
LVSVi	Left ventricular stroke volume indexed
m	Meter
mg/dL	Milligram per decilitre
MID	Middle
MOLLI	Modified Look-Locker inversion-recovery
mm	Millimetre
MMAVD	Mixed mitral and aortic valve disease
mm/h	Millimetres per hour
MMP - 1	Matrix metalloproteinase-1
MMVD	Mixed mitral valve disease
MR	Mitral regurgitation
MRAR	Mitral regurgitation and aortic regurgitation
MRI	Magnetic resonance imaging
ms	Milliseconds
MS	Mitral stenosis
MV	Mitral valve
n	Number
NSF	Nephrogenic systemic fibrosis
NYHA	New York Heart Association
PIP	Procollagen Type 1 C-peptide
PIIINP	Procollagen III N-terminal pro-peptide
PSIR	Phase-sensitive inversion recovery

PSGN	Post-streptococcal glomerulonephritis
PR	Pulmonary regurgitation
PS	Pulmonary stenosis
PV	Pulmonary valve
REMEDY	Rheumatic heart disease registry
RF	Radiofrequency
RHD	Rheumatic heart disease
ROI	Region of interest
RV	Right ventricle/right ventricular
RVEDV	Right ventricular end- diastolic volume
RVEDVi	Right ventricular end- diastolic volume indexed
RVEF	Right ventricular ejection fraction
RVESV	Right ventricular end- systolic volume
RVESVi	Right ventricular end- systolic volume indexed
RVOT	Right ventricular outflow tract
RVSVi	Right ventricular stroke volume indexed
SA	Short axis
SAPHIRE	Saturation pulse prepared heart-rate- independent inversion recovery
SASHA	Saturation recovery single-shot acquisition
SD	Standard deviation
shMOLLI	Shortened modified Look-Locker inversion-recovery
SPSS	Statistical Package for the Social Sciences
SSA	Sub-Saharan Africa
SSFP	Steady-state-free-precession

STIR	Short T-tau- inversion-recovery
SV	Stroke volume
SVC	Superior vena cava
TE	Echo time
TI	Inversion time
TNF	Tumour necrosis factor
TRr	Tricuspid regurgitation
TR	Repetition time
TS	Tricuspid stenosis
TV	Tricuspid valve
UCT	University of Cape Town
USA	United States of America
VO2 MAX	Volume Maximum volume of oxygen maximum consumption per unit time

ABSTRACT

INTRODUCTION: Rheumatic heart disease (RHD) is the major sequel of acute rheumatic fever (ARF) and occurs in approximately 60% of the cases. Globally, RHD is the most common acquired cardiovascular disease, affecting more than 15 million people per year, causing approximately 233,000 deaths. RHD remains a significant cause of heart failure in low- and middle-income countries, including sub-Saharan Africa, contributing to considerable morbidity and mortality, often affecting young economically active members of society.

OBJECTIVE: The aim of the study was to document the extent of myocardial fibrosis in subjects with RHD, in order to determine the degree of altered myocardial tissue characteristics using a multiparametric cardiovascular magnetic resonance (CMR) approach; assess left ventricular (LV) function and strain, and to assess focal and diffuse myocardial fibrosis in subjects with RHD.

METHODOLOGY: Enrolled subjects with a confirmed diagnosis of RHD, and age- and sex-matched healthy controls underwent CMR using a 3T Siemens Skyra (Erlangen, Germany) scanner. CMR parameters included steady-state-free-precession (SSFP) cine, cine tagging, T1-weighted imaging, T2 short Tau inversion-recovery (STIR), native T1 mapping (Modified-Look-Locker inversion recovery), T2 mapping and late gadolinium enhancement (LGE) imaging and extracellular volume (ECV) estimation.

RESULTS: Forty-four (44) subjects (mean age 42.8 ± 13.8 years; female 63.6%) with a confirmed diagnosis of RHD, and 30 age- and sex-matched healthy controls (mean age 38.87 ± 12.31 years; female 53.3%) were enrolled in the study. RHD subjects showed an increased indexed LV end-diastolic, end-systolic, and stroke volume and mass, compared to controls ($p = 0.001$). LV ejection fraction (LVEF) was reduced in the RHD cohort compared to controls (44.0 ± 13.26% versus 56.9 ± 5.19%, $p < 0.001$). There was significant left atrial dilatation in RHD subjects compared to controls (41.37 ± 11.84 mm versus 21.77 ± 3.13 mm, $p < 0.001$). Increased indexed RV end-diastolic, end-systolic and stroke volumes were found. RV ejection fraction was significantly lower in RHD subjects compared to controls (41.07 ± 16.19% versus 53.60 ± 7.46%, $p < 0.001$). Valvular lesions most commonly observed were mixed mitral valve disease (27%) and mixed mitral and aortic valve disease (43%). Native T1 values were

elevated in RHD subjects compared to controls (1279.98 ± 54.14 ms versus 1212.85 ± 33.34 ms, p = 0.004). T2 mapping values to assess oedema were normal, in both RHD subjects and controls (39.26 ± 2.92 versus 38.72 ± 2.19, p = 0.32); relative T2 STIR imaging parameters were 1.31 ± 0.34 versus 1.48 ± 0.22, p = 0.02.
Late gadolinium enhancement (LGE) was evident in all 44 (100%) RHD subjects, with linear (26%), patchy (36%) and diffuse (38%) patterns of enhancement. ECV values were elevated in RHD subjects compared to controls (0.36 ± 0.05 versus 0.28 ± 0.01 %, p < 0.001). Linear regression analysis showed moderate negative correlation between native T1 and peak diastolic circumferential strain rate (R = -0.412, p = 0.001) and strong correlation between ECV and peak diastolic circumferential strain rates (R = -0.43, p = 0.00).

CONCLUSION: This study showed a high prevalence of fibrosis throughout the myocardium in all RHD subjects, irrespective of valvular pathology. Increased native T1 and ECV indicate increased myocardial fibrosis. Normal signal intensity ratio on T2-weighted oedema imaging (STIR) and T2 values indicated absence of active inflammation in advanced, chronic RHD. These data, showing a high fibrotic burden, may provide an explanation for increased mortality in RHD as excess myocardial fibrosis has been strongly linked with mortality in other disease contexts.

KEYWORDS: Rheumatic heart disease, valvular lesions, acute rheumatic fever, left ventricular function, myocardial fibrosis, strain

CHAPTER ONE
STUDY OVERVIEW

1.1 Introduction

Acute rheumatic fever (ARF) occurs approximately 2 weeks after a throat infection with Group A Streptococcus pyogenes (GAS) typically affecting untreated genetically predisposed children between 5 and 15 years of age. Rheumatic heart disease (RHD) is the major sequel of ARF and occurs in approximately 60% of the cases (Martin et al., 2015).

RHD is a disease of poverty, related to overpopulation, suboptimal living circumstances and lack of access to health care facilities. Globally, RHD is the commonest acquired cardiovascular disease, affecting more than 15 million people annually, causing approximately 233 000 deaths (Beaton et al., 2012; Remenyi et al., 2013; Mayosi, 2014). RHD is a significant cause of heart failure in low- and middle-income countries (LMICs), including sub-Saharan Africa (SSA), contributing to significant morbidity and mortality, often affecting young economically active members of society (Remenyi et al., 2013). Following a period of significant global policy inactivity on RHD, there has been a rebirth in research in recent years to address this disease of poverty (Abouzeid et al., 2019).

Cardiovascular magnetic resonance (CMR) has several advantages in the imaging of RHD. First, CMR is reproducible and accurate. Second, it is safe for the study of RHD. Third, it allows for the study of tissue characteristics, including inflammation and fibrosis, which are pathophysiologically important in RHD. Finally, CMR is the gold standard modality for assessment of cardiovascular anatomy and global and regional myocardial function (Ntusi, et al., 2015; Neubauer, 2018).

There is a paucity of studies conducted in subjects with RHD using multiparametric CMR. It is in this context that a need arises to investigate the role of a multiparametric CMR in subjects with chronic RHD. This chapter will provide a brief overview of the rationale of the research study, highlight the value of using CMR to characterise the features of RHD.

1.2 Rationale

Acute myocardial injury was historically visualised by using multiple tissue characterisation techniques such as T1-weighted (T1W) and T2-weighted (T2W) imaging for oedema assessment, and LGE for focal fibrosis assessment (Friedrich et al., 2009). LGE is efficacious in producing excellent contrast between diseased and normal myocardium and demonstrates different enhancement patterns and distribution to distinguish between different causes of focal necrotic/scarred myocardium, including the differentiation between ischaemic and nonischaemic aetiologies (Friedrich et al., 2009). However, there are constraints when using LGE in isolation for the diagnosis of diffuse myocardial injury. In some subjects, global oedema may be demonstrated without overt myocyte necrosis, leading to negative findings on LGE imaging. Second, to detect focal myocardial injury using LGE a normal myocardium is required as a reference for comparison. In absence of a normal myocardium, LGE does not always perform well for diffuse fibrosis. In addition, although gadolinium-based contrast media poses a minimal risk, these agents are linked to the rare but serious consequence of nephrogenic systemic fibrosis (NSF) when used in subjects with significant impaired renal function. Therefore, it would be useful to employ a method with high sensitivity to display the different changes in myocardial injury without the administration of gadolinium (Friedrich, 2016). T1 myocardial mapping may be performed with or without contrast.

1.3 Research Problem

RHD is the chronic manifestation occurring because of pancarditis from ARF involving both the myocardium and heart valves (Zühlke et al., 2014). Diagnosis of ARF is based on a set of guidelines, known as the Modified Jones criteria, which consist of major and minor criteria. Diagnosis of ARF requires the presence of either 2 major criteria, or 1 major and 2 minor criteria combined with the evidence of streptococcal infection, elevated or increasing anti-streptolysin O titre (ASOT) or anti-deoxyribonuclease B (anti-DNase B) levels (Beaton & Carapetis, 2015). The American Heart Association (AHA), in 2015, published a revised version of the Jones criteria, highlighting the importance of including subclinical carditis to the list of major criteria and added echocardiography as a diagnostic tool. Inclusion of echocardiography ensured detection of clinically silent valvular involvement as an indicator of ARF (Beaton & Carapetis, 2015).

Cardiovascular manifestations of ARF may include various degrees of carditis including myocarditis, endocarditis and pericarditis, with associated valvular incompetence, left ventricular (LV) dysfunction, arrhythmia and heart failure. Subjects with chronic RHD may have valvular stenosis, with valve regurgitation, LV dysfunction, arrhythmia and premature mortality (Gewitz et al., 2015; Mutnuru et al., 2016). It has been postulated that chronic RHD has a phenotype of subclinical inflammation and diffuse myocardial fibrosis that is reactive to ongoing tissue inflammation (Suthahar et al., 2017). In this study, LGE and parametric mapping was employed to perform a quantitative and qualitative assessment of the degree of myocardial fibrosis in subjects with RHD. The use of LGE, CMR T1 mapping (before and after contrast media administration), extracellular volume (ECV) quantification, as well as T2 mapping, enabled quantitative assessment of the tissue characteristics related to RHD in a non-invasive manner.

1.4 Research Question

The primary research questions for this study were as follows:

1. To what extent does RHD cause left ventricular (LV) functional abnormalities?
2. With what degree of accuracy can diffuse myocardial fibrosis be diagnosed using CMR in RHD subjects?
3. What is the degree of myocardial strain abnormalities in subjects with RHD?

1.5 Aim

The aim of the study was to document the extent of myocardial fibrosis and inflammation in subjects with RHD by utilising multiparametric CMR imaging characterisation.

1.6 Objectives

The objectives for this study were to:

1.6.1 assess the extent of valvular disease in subjects with RHD

1.6.2 assess LV function in subjects with RHD

1.6.3 assess strain abnormalities in RHD

1.6.4 assess focal and diffuse myocardial fibrosis in RHD

1.7 Summary

RHD is associated with myocardial inflammation, fibrosis and valvular insufficiency. CMR is the gold standard for investigating the heart in a comprehensive and non-invasive manner using LGE for the detection of focal myocardial fibrosis. However, LGE relies on comparing areas of scarring to normal myocardium by visual assessment and is therefore limited in the detection of diffuse myocardial fibrosis (Ntusi et al., 2015). In view of this, the researchers sought to investigate the combination of LGE imaging and T1 mapping prior to and following gadolinium-based contrast administration to quantify the extent and pattern of myocardial fibrosis in RHD.

1.8 Thesis overview

Chapter 2 provides an in-depth discussion of the literature on RHD epidemiology, pathophysiology, morbidity, mortality and treatment strategies. The application of dedicated CMR sequences is discussed to facilitate the assessment of cardiac structure and function. The chapter concludes with a review of literature on CMR in patients with ARF and RHD.

In Chapter 3, a description of the research design and methodology is provided. In addition, the ethical considerations relevant for this study, the recruitment strategy employed, sampling techniques, the data acquisition as well as data analysis will be discussed.

Chapter 4 provides a detailed report of the results of this study. The results are presented in the form of graphs, tables and diagrams. The different data acquired pertaining to the objectives will be outlined.

Chapter 5 presents a discussion of the findings and concludes with a brief summary and the implications the findings have for imaging of RHD. Results will be juxtaposed with other research findings.

Chapter 6 summarizes the key findings of the study and provides recommendations for future research studies.

CHAPTER TWO
LITERATURE REVIEW

2.1 Chapter introduction

This chapter introduces the background for the research described in this thesis. Relevant literature will be explored to obtain a better understanding of how RHD affects the heart and the burden it places on society. This literature review will focus on CMR as a reliable and non-invasive diagnostic tool for the diagnosis of RHD.

2.2 Epidemiology

RHD contributes significantly to the burden of cardiovascular morbidity and mortality (Luiza & Jorge, 2013), and remains the most prevalent cause of acquired cardiovascular disease in children, adolescents and young adults in LMICs such as South Africa (Zühlke et al., 2015).

SSA is globally the region with the highest incidence of RHD. A study conducted at a school in Soweto in 1974, using auscultation to determine the diagnosis, reported an incidence of 5.9 per 1000 in asymptomatic school children (Zühlke et al., 2014). However, auscultation is a poor technique for detecting RHD, and echocardiography has proven to be more sensitive and reliable (Dougherty et al., 2017). Incidence of ARF is more than 10 per 100,000 in parts of Asia, the Middle East, Eastern Europe, and the Pacific regions (Seckeler & Hoke, 2011; Karthikeyan et al., 2017). The incidence of RHD in school going children in Mozambique, detected by echocardiography, has recently been predicted to be as high as 30.4 per 1,000. Further, recent estimations suggest that globally approximately 62 to 78 million people could have RHD, which would translate approximately 1.4 million deaths annually from RHD and its complications (Karthikeyan et. al., 2017).

2.3 Morbidity and mortality related to rheumatic heart disease

Morbidity and mortality associated with RHD is considerable. Approximately 233,000 - 468,164 people die from RHD every year. The long-term effects of RHD which include atrial fibrillation (AF), heart failure, stroke and infective endocarditis disable hundreds of thousands of individuals worldwide (Remenyi, B. et al., 2013). Prior to secondary penicillin prophylaxis use, the USA experienced a 20-year mortality, caused by ARF

and RHD, of between 30 - 80%, with most deaths before the age of 30 years (Remenyi et al., 2016).

High morbidity and mortality from ARF and RHD remain in LMICs, with a 3.0 - 12.5% mortality rate per annum. The mean age of affected individuals is younger than 25 years, with major concerns related to heart failure, infective endocarditis, AF, complications related to pregnancy and stroke (Remenyi et al., 2016).

The Rheumatic Heart Disease Registry (REMEDY) study, a comprehensive, prospective international, multicentre study, conducted in 25 health care facilities in Africa, India and Yemen, was designed to accumulate a current cohort of RHD patients from LMICs. Results showed that from a cohort of 3,343 patients, 63.9% presented with moderate-to-severe multivalvular disease complicated by congestive heart failure in 33.4%. Further complications were pulmonary hypertension (28.8%), AF (21.8%), stroke (7.1%), infective endocarditis (4%), and major bleeding in 2.7% of patients (Zühlke et al., 2015; Remenyi et al., 2016). Decreased LV systolic function was observed in 25% of adults and 5.3% of children. The LV was dilated in 23% of adults and 14.1% of children (Zühlke et al., 2015).

A study conducted, in 2013, at the Indira Gandhi Institute of Cardiology, Patna, reported that out of 972 deaths, 120 (12.34%) were caused by RHD. Either single severe valvular lesion or a combination of severe valvular lesions was found in 70 (58%) of these patients (Prasad et al., 2017).

The figure below shows the global prevalence and mortality rates of RHD. As can be noted form this figure, many African countries, including South Africa have a high prevalence for RHD.

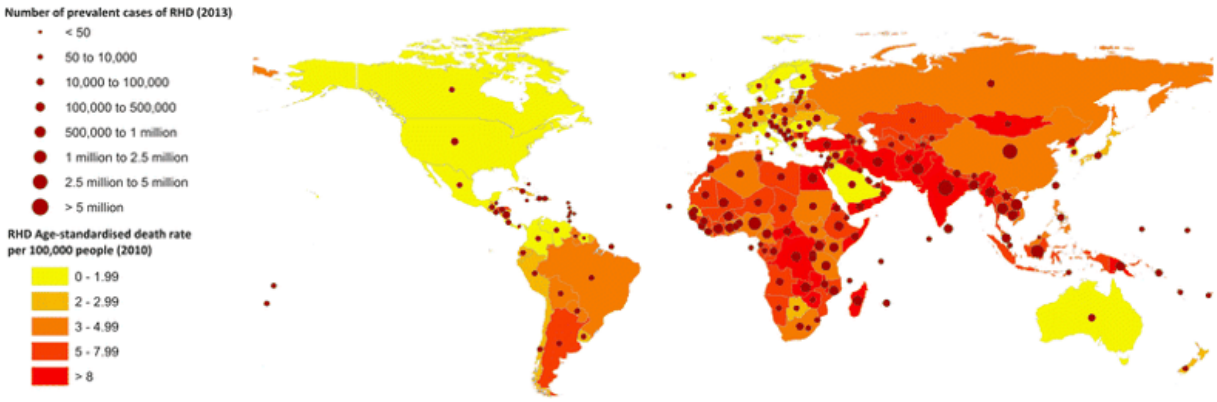

Figure 2.1: Global prevalence and mortality rates of rheumatic heart disease (Adopted from: Zühlke et al., 2017)

2.4 Pathophysiology of acute rheumatic fever/rheumatic heart disease

ARF and RHD are autoimmune conditions, that arise as a consequence of GAS infection of the throat and skin in susceptible children and young adults (Zühlke et al., 2017). GAS is anaerobic, gram-positive and only manifests in humans. The primary sites of colonisation are the oropharynx and the skin. GAS can cause both infectious and postinfectious immune-mediated diseases. Infections can be subdivided into non-invasive, including impetigo and pharyngitis; invasive infections, such as septic arthritis, pneumonia and necrotising fasciitis; and toxin-mediated syndromes, such as scarlet fever and toxic shock syndrome. Postinfectious immune-mediated diseases caused by GAS include ARF, RHD, post-streptococcal glomerulonephritis (PSGN) and paediatric auto-immune neuropsychiatric disorders (Martin et al., 2015). The pathophysiology of RHD commences with cross-reactive antibodies binding to cardiac tissue which cause infiltration of streptococcal primed $CD4^+$ T cells (Galvin et al., 2000; Guilherme et al., 2007). This triggers an auto-immune response, which releases inflammatory cytokines, such as tumour necrosis factor (TNF) alpha and interferon (IFN) gamma. $CD4^+$ T cells produce interleukin-4 (IL-4), present in valvular tissue causing valvular lesions due to persistent inflammation (Chin & Hackett, 2019).

In severe cases of ARF, the heart becomes dilated and can lead to death in the acute stage of the disease. The heart exhibits a non-specific myocarditis at autopsy, in which

lymphocytes and macrophages predominate (Rubin, 2001). Fibrinoid degeneration of collagen, in which the fibres become swollen and eosinophilic is characteristic. Several weeks after the onset of the disease, the Aschoff body, which is the typical lesion of rheumatic myocarditis, starts to develop. Initially the Aschoff body consists of a perivascular focus of swollen eosinophilic collagen surrounded by lymphocytes, plasma cells and macrophages (Rubin, 2001). In time, the structure becomes granulomatous in appearance, with a central fibrinoid focus being associated with a perimeter of lymphocytes, plasma cells, macrophages, and giant cells. The Aschoff body is eventually replaced by a nodule of scar tissue (Rubin, 2001).

2.5 Acute rheumatic fever

Clinical diagnosis of ARF is based on the revised Jones Criteria. The latter consists of a list of major and minor criteria, determined by the American Heart Association (AHA) (Gewitz et al., 2015).

2.5.1 Major criteria:

The 5 major manifestations of ARF are as follows:

i) ***Synovium – inflammatory arthritis*:** This is an inflammatory process which affects major joints such as the knees, ankles, elbows and wrists. Rapid response to salicylates and nonsteroidal anti-inflammatory drugs is typical of the disease and symptoms usually last for approximately 4 weeks (Gewitz et al., 2015).

ii) ***Heart - Endocarditis***: The heart valves mainly affected by ARF include the mitral and aortic valves. Inflamed valves have a finely nodular, wart-like or verrucous appearance at the line of closure. Inflammation sets in around the areas of the valve where there is focal loss of collagen resulting in ulceration of the surface of the valve and fibrin deposits which causes the verrucous lesions (Rubin, 2001).

iii) ***Heart - Carditis***: Carditis is diagnosed in approximately 50% of ARF cases and usually occurs a few weeks following infection. Patients usually present with valvulitis, sometimes in combination with pericarditis or myocarditis (Marijon et al., 2012). Signs of acute carditis may include a heart murmur, sinus tachycardia, and a soft first heart sound related to a consistent prolonged PR interval demonstrated on an electrocardiogram (ECG) (Marijon et al., 2012).

iv) ***Brain – chorea*:** Sydenham's chorea is a neurological condition which is characterised by spontaneous, rapid and random movement of the face and limbs (Martin et al., 2015; Zühlke et al., 2017). Sydenham's chorea may clinically appear with other features of ARF, but presentation is delayed, often as long as 6 months after infection ((Martin et al., 2015).

v) ***Skin – erythema marginatum and subcutaneous nodules:*** Erythema marginatum is identified by an atypical, fading, pink rash and has a similar appearance as ringworm. The areas that are commonly affected are the torso, upper arms and legs, and, very rarely, the face (Gewitz et al., 2015). Specific joints such as the knees, elbows and wrists are common sites where subcutaneous nodules can be observed (Martin et al., 2015). These solid, painless bulges can also be observed in the occipital region and laterally to the spinous processes of the thoraco-lumbar vertebrae (Gewitz et al., 2015).

2.5.2 Minor criteria for low-risk populations include the following symptoms:

- Polyarthralgia
- Temperature ≥ 38.5°C
- Erythrocyte sedimentation rate (ESR) ≥ 60 mm in the first hour and/or C-reactive protein (CRP) ≥ 3.0 mg/dL§ ESR ≥ 30 mm/h and/or CRP ≥ 3.0 mg/dL§
- Prolonged PR interval on ECG after accounting for age variability (Gewitz et al., 2015).

Low risk populations have an ARF prevalence < 2/ 100,000 in school-going children per annum, or an occurrence of RHD ≤ 1/1,000 inhabitants, in all ages, per annum (Beaton & Carapetis, 2015).

2.5.3 Minor criteria for high-risk populations include the following symptoms:

- Monoarthralgia
- Temperature ≥ 38.5°C
- ESR ≥ 30 mm/h and/or CRP ≥ 3.0 mg/dL§
- Prolonged PR interval on ECG, excluding carditis as a major criterion and depending on age variability (Gewitz et al., 2015)**.**

High-risk groups are defined as people residing in societies with high prevalence of ARF (incidence > 30/100,000 per year in 5 to 14-year olds) or RHD (all-age prevalence > 2/1000) (RHD Australia, 2012).

Based on the revised Jones Criteria for the diagnosis of ARF, a positive diagnosis of ARF requires the presence of either 2 major criteria only, or 1 major and 2 minor criteria combined with the evidence of streptococcal infection, elevated or increasing antistreptolysin O titer (ASOT) or anti-deoxyribonuclease (DNAse) B levels (Gewitz et al., 2015).

2.6 Rheumatic heart disease

Diagnosis of RHD is not always preceded by clinically manifest ARF; and in most cases patients present between ages 20 to 50 years, with symptoms of heart failure. There is evidence of increased disease prevalence amongst women, which is ascribed to hormonal, autoimmune and socioeconomic factors, including child-rearing, which could be the cause of repeated exposure to group A-streptococcus. Other factors include difficult access to healthcare facilities as well as genetic predisposition to autoimmune diseases (Marijon et al., 2012).

2.6.1 Valvular disease

Although RHD may be a form of pancarditis, involving the entire heart, it mainly affects the endocardium and recurring episodes of autoimmune reactions result in chronic inflammation and scarring of the heart valves (Zühlke et al., 2014). The valves most commonly affected in RHD are the mitral and aortic valves. This may be due to their structure which is made up of a small core of connective tissue surrounded by two layers of endothelial tissue (Remenyi et al., 2016). Although histopathology shows that the mitral valve is generally affected by RHD, isolated aortic valve involvement has been reported in approximately 2% of patients (Remenyi et al., 2016).

Both mitral stenosis and mitral regurgitation can occur in RHD, and mixed mitral valve disease is common. Mitral valve stenosis occurs due to ongoing or repeated inflammation with bi-commissural fusion. Patients with mitral regurgitation may remain asymptomatic for several years due to dilatation of the left atrium and ventricle which precedes LV systolic dysfunction to compensate for the mitral incompetence (Marijon et al., 2012). Although aortic stenosis can be confined and severe, there is a strong

correlation to mitral regurgitation (Marijon et al., 2012). Tricuspid and pulmonary valve involvement is only, and rarely, seen in patients with advanced disease (Remenyi et al., 2016). The main cause for functional tricuspid regurgitation (TRr) is mitral stenosis with raised pulmonary pressures and resultant right ventricular (RV) dilatation (Marijon et al., 2012).

Several post-inflammatory cytokines are involved in the pathogenesis of post streptococcal immune syndromes. Increased plasma or serum IL-1α, IL-2, IL-6, IL-8 and TNF have been reported in patients with ARF and RHD (Martin et al., 2015). However, reduced levels of IL-1, IL-2, TNF and immunoglobulin production, have been found in tonsillar cells isolated from RHD, following T cell activation (Guilherme et al., 2007; Martins et al., 2017).

Mitral valve apparatus undergoes primary morphological change as a result of rheumatic mitral regurgitation. In turn, dilatation of the LV and eccentric hypertrophy in mitral regurgitation are secondary remodelling phenomena as a complication of haemodynamic volume overload on the LV produced by primary change in the morphology of the mitral valve in RHD. The mitral valve becomes thickened after the onset of inflammation and fusion of the leaflets at the commissures sets in, which has an impact on valve motion in both systole and diastole. Adaptive LV dilatation occurs as a result of mitral regurgitation causing an increase in end-diastolic volume. The eccentric LV hypertrophy aids with maintaining high stroke volumes. However, in the decompensated phase, advanced dilatation of the ventricle results in increased wall strain with tissue damage and abnormal contractility (Marciniak et al., 2007; Gaasch & Meyer, 2008; Banerjee et al., 2014). Acute inflammation may lead to rapid decline of cardiac function, whereas chronic inflammation can cause advanced structural damage, resulting in cardiac fibrosis (Suthahar et al., 2017).

Rheumatic valvular disease is the cause of significant morbidity occurring as a result of cardioembolic stroke, AF, congestive failure, and infective endocarditis (Karthikeyan et al., 2017). In a study by Carapetis et. al., (2005) it was estimated that approximately 7.5% of all strokes occurring in LMIC's, could be as a direct consequence of RHD.
RHD also has a negative effect on the outcomes of pregnancy. In approximately 10.4% of South African women who demised during pregnancy, more than half had RHD as a pre-existing condition. RHD and its complications lead to substandard living

conditions due to loss of income; in children it causes poor performance at school (Moodley et al., 2000; Karthikeyan et al., 2017).

2.7 Treatment

The treatment strategy for ARF and RHD is primarily preventative and can be divided into various categories namely; community based, primary and secondary prevention. Prevention of ARF can be achieved by treating throat infections with penicillin to eradicate GAS. Safety and efficacy of penicillin prophylaxis has been well-established and can be combined with improvement in socio-economic conditions, which include living conditions, education and awareness (Marijon et al., 2012 **;** Zühlke & Engel, 2013).

2.7.1 Community-based prevention

Access to healthcare facilities, hygiene and living conditions play a pivotal role in the prevention and treatment of RHD and its precursor. High-income countries such as the USA and Western Europe have shown a decrease in the occurrence of ARF even before the antibiotic era, due to better socio-economic development. However, better socio-economic conditions are not necessarily the best preventative measure to protect patients from contracting the disease (Marijon et al., 2012).

2.7.2 Primary prevention

Randomised controlled trials conducted in the 1950s confirmed that ARF could be prevented by treating GAS pharyngitis with penicillin. GAS infection can be deracinated by screening active sore throat and treating pharyngitis with oral antibiotics (Zühlke & Engel, 2013). The efficacy of primary prophylaxis in the treatment of high-risk populations, was proven by a study conducted on army personnel in the USA. After this, the Baltimore-based program, showed a 50-fold decline in the incidence of ARF after 15 years. The latter consisted of a comprehensive program that was focussed on diagnosing and treating streptococcal infections in children from the city (Zühlke & Karthikeyan, 2013).

2.7.3 Secondary prevention

The aim of secondary prevention is to reduce the incidence of new GAS strains that might lead to recurring ARF. Recrudescence plays a vital role in cardiac outcome (Marijon et al., 2012). A single injection of benzathine benzylpenicillin every 3-4 weeks

is recommended after ARF. This has proven to be more effective compared to oral treatment. Factors affecting the period of treatment are age, the date of the previous attack, and the presence and severity of RHD. Risk of recurrence in highly endemic areas proves to be high and therefore some healthcare institutions have implemented permanent prophylaxis for patients with severe RHD or history of prior valvular surgery (WHO, 2001; Marijon et al., 2012; Irlam et al., 2013; Gewitz et al., 2015). The delivery of secondary prophylaxis is more efficient in areas with community-based registry programmes compared to those without a registry (McDonald et al., 2005; Marijon et al., 2012). The efficiency of such a program depends highly on resources such as education, involvement of health care workers within the community as well as existing primary care networks (Marijon et al., 2012 ; Moxon et al., 2017).

2.7.4 Treatment of rheumatic heart disease

Surgical valve replacement remains the cornerstone of treatment for patients with established RHD (Zühlke et al., 2017). Treatment for patients who have symptoms of heart failure includes mainly diuretics, beta blockers and angiotensin-converting-enzyme inhibitor therapies. Complications such as AF require rate or rhythm control and anticoagulation with warfarin for those who are at high risk of embolic complications (Marijon et al., 2012).

2.8 Cardiovascular magnetic resonance

CMR is a medical imaging technique which enables the assessment of the structure and function of the cardiovascular system, in a non-invasive manner. Image acquisition is formed on the same basis as magnetic resonance imaging (MRI) but sequences are optimised to meet the requirements of the cardiovascular system. These optimisations are primarily in the use of electrocardiographic (ECG) -vector gating and rapid imaging techniques or sequences to avoid artefacts due to respiration and movement of the heart (Nacif et al., 2012). Static CMR images are acquired during a single part of the cardiac cycle and use the intrinsic contrast in the tissues to demonstrate pathology in order to make a diagnosis. Cine images involve a series of images acquired through different phases of the cardiac cycle to record cardiac motion or blood flow (Myerson et al., 2010). By combining various techniques to create protocols, one can assess the key functional and morphological features of the cardiovascular system (Nacif et al., 2012). CMR is the imaging modality of choice for the non-invasive assessment of

myocardial inflammation in patients with suspected myocarditis (Friedrich & Marcotte, 2013).

2.8.1 Electrocardiographic gating

CMR has two fundamental challenges, namely motion of the lungs during respiration and motion of the heart during the cardiac cycle. Respiratory motion is circumvented with breath holding during image acquisition, whereas cardiac motion is controlled by using electrocardiographic (ECG) gating (Norton et al., 2013). There are 2 ways in which data acquisition can be synchronised to the cardiac cycle, namely prospective gating and retrospective gating.

2.8.1.1 Prospective gating

Prospective triggering allows for data to be obtained during a predetermined period of the cardiac cycle, namely diastole.

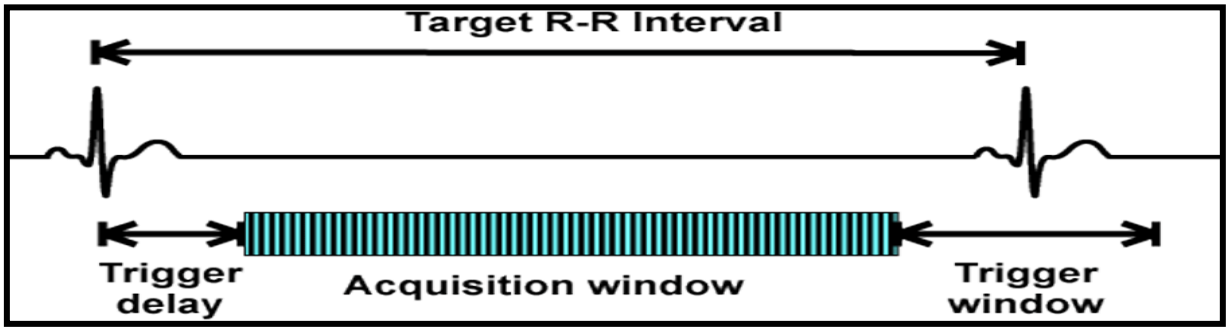

Figure 2.2: Cine images are acquired using a prospectively gated technique during diastole, the resting phase of the cardiac cycle (represented by the acquisition window in above diagram). (Adopted from Elster, 2015)

The R-wave of the ECG is the most stable indicator of the onset of systole and is used as a reference point for data acquisition which is started following a given delay after the R-wave. An important caveat of this method is the fact that image acquisition does not include the entire RR interval which may result in stroke volumes being underestimated in the volume analysis. Prospective gating for morphological imaging takes place during mid-diastole which occurs between the T-wave (cardiac repolarisation) and the A-wave (atrial contraction) (Nacif et al., 2012).

2.8.1.2 Retrospective gating

This approach allows for data to be collected during all the cardiac phases (systole and diastole) and then retrospectively assigned to the cardiac cycle (Elster, 2015).

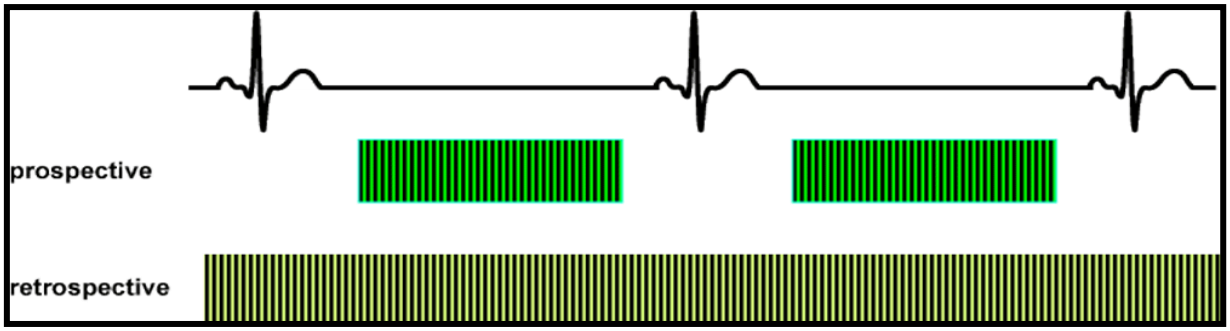

Figure 2.3: A comparison of prospective gating (green bars at the top) and retrospective gating (bars at the bottom) techniques. Note that the images are acquired during the entire cardiac cycle during retrospective gating.
(Adopted from Elster, 2015)

One of the major advantages of the retrospective gating method is that it collects data from all the cardiac phases. However, one of the major challenges of this technique is data acquisition in the presence of arrhythmias and low amplitude R-waves. The latter results in an unequal change in the systolic and diastolic periods. As a result of this, retrospective software is unable to perform proper segmentation of the cardiac phase data (Elster, 2015).

2.8.2 Basic physics of magnetic resonance

2.8.2.1 The components of the magnetic resonance imaging scanner

MRI hardware comprises the electrical and mechanical components of a scanning device. The main hardware components of the MRI scanner include the following:

2.8.2.2 The superconducting magnet

The main component of the MRI scanner is the magnet. The magnet consists of miles of superconducting wire, wound in rings, immersed in a liquid bath of helium (He). The He is kept at extremely low temperatures (approximately -269°C) to cool down these wires. Superconductivity refers to the phenomenon of scanner, once connected to a power source, being able to conduct electricity indefinitely, even when disconnected from the power source (Myerson et al., 2010).

2.8.2.3 The gradient coils

The scanner consists of 3 sets of gradient coils, one in each (x, y, z) direction. Their function is to produce deliberate variations in the main equilibrium magnetic field or B_0. This variation allows the localisation of the different image slices, namely axial, coronal and sagittal without moving the subject as well as phase and frequency encoding (Myerson et al., 2010).

2.8.2.4 The radiofrequency coils

MR experiments rely on the transmission of radiofrequency (RF) excitation pulses, at the resonance frequency, to excite the hydrogen protons in the body. The subject then emits an RF signal that is received and measured by the surface coil. RF antennae are responsible for the transmission of the excitation pulses and signal reception. These antennae are commonly referred to as the RF coils. The main RF coil, also known as the body coil, is situated within the bore of the magnet (Smith & Lange, 1997).

2.8.3 Signal creation

Image formation in MRI is primarily dependent on the inherent magnetic properties of the human tissue which is used to create tissue contrast (Duran et al., 2013). The human body consists mainly of water, present in organs such as the brain, heart, kidneys and skin, as well as in bones and muscle (Duran et al., 2013). All these tissues have abundant hydrogen atoms - approximately 63% (Duran et al., 2013). Atoms are made up of a nucleus, which consists of protons and neutrons and a shell which consists of electrons. Protons have a positive electrical charge, and they possess a spin. This results in electrical current being created and an electrical current induces magnetic force or a magnetic field (Westbrook et al., 2005).

Image formation in CMR is based on the relaxation of protons in the hydrogen nucleus. The latter is specifically characterised by 2 parameters, namely:

(1) The longitudinal relaxation time (T1) or spin-lattice relaxation time. The T1 relaxation time is determined by the speed at which protons can recover at least 63% of its longitudinal equilibrium value (Westbrook et al., 2005). T1 differences are emphasised in imaging sequences such as T1-weighted fast spin echo, with a short repetition time (TR), used for tissue characterisation (Myerson et al., 2010).

(2) The transverse, or spin-spin relaxation time (T2) (Westbrook et al., 2005). This is a constant expressing the time it takes for transverse magnetisation to decay to e^{-1}, or approximately 37% of its original value (Greenwood et al., 2015). Both T1 and T2 are measured in milliseconds. Methods that are emphasised by T2 differences include T2-weighted fast spin echo, with a long echo time (TE) as well as the sequence used for the acquisition of cine images, such as the steady-state-free-precession (SSFP) sequence (Myerson et al., 2010).

2.8.3.1 Inversion recovery

Inversion recovery (IR) sequence is used to assess late gadolinium enhancement (LGE). It exploits the varying T1 properties of tissues. An RF pulse, which inverts the magnetisation of the spins, is applied, which returns to their original state at rates dependent on their T1. If imaging takes place before the spins have fully regained their equilibrium, it can emphasise the differences in equilibrium. The time taken between the application of the inversion pulse and image acquisition is referred to as the inversion time, or TI (Myerson et al., 2010).

2.8.3.2 Late gadolinium enhancement imaging

The concept of LGE is based on the delay in wash-in and wash-out of gadolinium in tissues with an increased proportion of extracellular space, compared to the rapid wash-in and wash-out in normal tissues (Doltra et al., 2013; Franco et al., 2015). In the presence of acute myocardial injury, LGE is a result of cellular necrosis and lysis, and oedema. Whereas, in the instance of chronic infarction, the fibrous scar tissue with its increased extracellular space is the basis (Doltra et al., 2013). T1-weighted imaging is used to demonstrate the presence of gadolinium in the myocardium, in the time period of 5 – 30 minutes after administration (Doltra et al., 2013).

2.8.3.3 Parametric mapping

The use of T1 and T2 mapping as a quantitative measure of tissue characterisation has undergone further development and is currently a robust technique applied in everyday clinical practice in multiple centres (Neubauer, 2018).

2.8.3.3.1 T1 mapping

T1 mapping quantifies the T1 (longitudinal or proton spin-lattice) relaxation time of a specific tissue, such as the myocardium, without employing a gadolinium-based

contrast agent (GBCA), on a pixel-by-pixel basis (Germain et al., 2014). The T1 relaxation time, measured in milliseconds (ms), differs from one tissue to the next, and is influenced by the magnetic field strengths (1.5T – 3T) and is also site specific (Bulluck et al., 2015). Various techniques are available to perform T1 mapping. All of these are derived from the electrocardiographically (ECG) gated inversion-recovery (IR) sequence, which includes the Look-Locker (LL) sequence, the Modified Look-Locker inversion-recovery (MOLLI) and the Shortened Modified Look-Locker inversion-recovery (ShMOLLI) sequence. Additional sequences have been developed for T1 mapping, namely saturation pulse prepared heart-rate- independent inversion recovery (SAPHIRE) and saturation recovery single-shot acquisition (SASHA). A single breath-hold, over 10-heartbeats, is required to acquire the SASHA sequence. The accuracy of this sequence does not depend on parameters such as absolute T1, heart rate, and flip angle, however it has lower accuracy compared to the MOLLI sequence. SAPHIRE sequences employ saturation and inversion pulses to create a T1 map with an amplified dynamic range, but, similar to SASHA, has lower accuracy compared to MOLLI (Cannaò et al., 2016).

The LL sequence consists of approximately 20 images, which enable an inversion time (TI) that is suitable for nulling of the myocardium. The TI usually ranges between 200 and 300 ms. These images are then post-processed to create a voxel-by-voxel map for T1 values (Cannaò et al., 2016). A limitation of this technique is the inconsistency in heart rates and it does not allow image acquisition at varying phases of the cardiac cycle (Cannaò et al., 2016). The shortened MOLLI (ShMOLLI) sequence overcomes these heart rate variability challenges. The MOLLI, derived from the LL sequence, was used in this study. T1 maps are generated from images that are acquired from 3 sequential IR pulses into a single data set. Data is captured at a fixed point in the cardiac cycle over 11 heart beats per breath-hold for each T1 map slice (Cannaò et al., 2016). A further limitation of this technique is that voxel-by-voxel estimation of the T1 can be compromised by the movement of the myocardium due to respiration and heart beats between frames. However, this can be overcome by motion correction algorithms (Cannaò et al., 2016). The MOLLI sequence enables an accurate and reproducible in vivo measurement of the myocardium.

2.8.3.3.2 T2 mapping

T2 mapping technique is based on the acquisition of 3 T2-prepared SSFP images, each acquired with a varying T2 preparation time. Images are acquired in the transient mode of single-shot SSFP directly after T2 preparation. The signal in each image is influenced by the T2 preparation and hence, signifies a different echo time along the T2 decay curve, which allows the calculation of the T2 relaxation times of each image pixel (Cannaò et al., 2016).

2.8.3.3.3 Postcontrast T1 mapping for extracellular volume quantification

Gadolinium based contrast agents (GBCAs) possess paramagnetic properties that shorten the T1 relaxation time of tissues. The molecular size of the contrast agent allows distribution in the extracellular space without invasion of the healthy myocytes. Certain diseases may either cause expansion of the extracellular space or disrupt the myocardial cell membranes. This results in an increase in the volume of distribution of the GBCA causing gadolinium enhancement (Doltra et al., 2013). The extracellular matrix (ECM) is made up of an intricate architectural network of structural and non-structural proteins. The latter serve to strengthen the ECM and adds to its elasticity. Extracellular volume (ECV) pertains to the measurement of the extracellular fluid that hydrates the ECM. In certain conditions such as fibrosis and oedema, the ECM and ECV may expand. The extracellular space is only partially measured in postcontrast T1 mapping because GBCAs do not cross cell membranes (Doltra et al., 2013). Postcontrast T1 mapping values are influenced by certain confounding variables such as glomerular filtration rate, gadolinium dose, time point at which maps are acquired post contrast, haematocrit level as well as body composition (Roller et al., 2015). A reliable approach to measure ECV is by subtracting pre- and postcontrast maps with haematocrit correction, which is usually obtained approximately 15 minutes after the administration of contrast. The formula used is as follows:

ECV = (1 – haematocrit) * (1 / T1 myocardium post-contrast – 1 / T1 myocardium pre-contrast) / (1 / T1 blood post-contrast – 1 / T1 blood pre-contrast) (Roller et al., 2015).

2.9 Role of cardiovascular magnetic resonance in rheumatic heart disease

Myocardial LGE was originally validated using GBCAs and found to be useful in the identification of focal fibrosis. In recent years, native T1 and T2 mapping techniques have been employed which prove to be more reliable in the diagnosis of inflammation and acute injury. In addition, native T1 is important for myocardial characterisation in

infiltration and fibrosis. Postcontrast T1 mapping and estimation of ECV is useful to determine the degree of diffuse myocardial fibrosis. CMR studies have been used in small case series and case reports to aid in the diagnosis and management of patients with RHD (Ntusi, 2018; Baebler & Emrich, 2018). Sepulveda and colleagues evaluated 18 patients with ARF using LGE to detect myocardial inflammation and injury. These authors reported pericardial effusion and mitral valve thickening in all 18 patients, aortic valve thickening in 17, RV dysfunction in 8 and LV dysfunction in 5 patients. LGE was present in all patients and was found to be diffuse, mesocardial and heterogeneous (Sepulveda et al., 2013).

In 2016, a group of researchers at this facility conducted a case study in a young woman who presented with heart block, using CMR (Fig. 2.4). The findings showed normal global biventricular function, however, peak circumferential systolic and diastolic strain rates were impaired. T2-weighted imaging showed increased signal intensity ratio and elevated T1 and T2 times, which supported the evidence of myocardial oedema. LGE imaging revealed no evidence of myocardial fibrosis, but striking enhancement of the valves indicative of valvulitis. (Fig. 2.4) In this study, a diagnosis of ARF was further supported by elevated ASOT levels (172 mmol/L) and elevated serum anti-DNAse B levels (370 mmol/L) in the patient (Samuels et al., 2017).

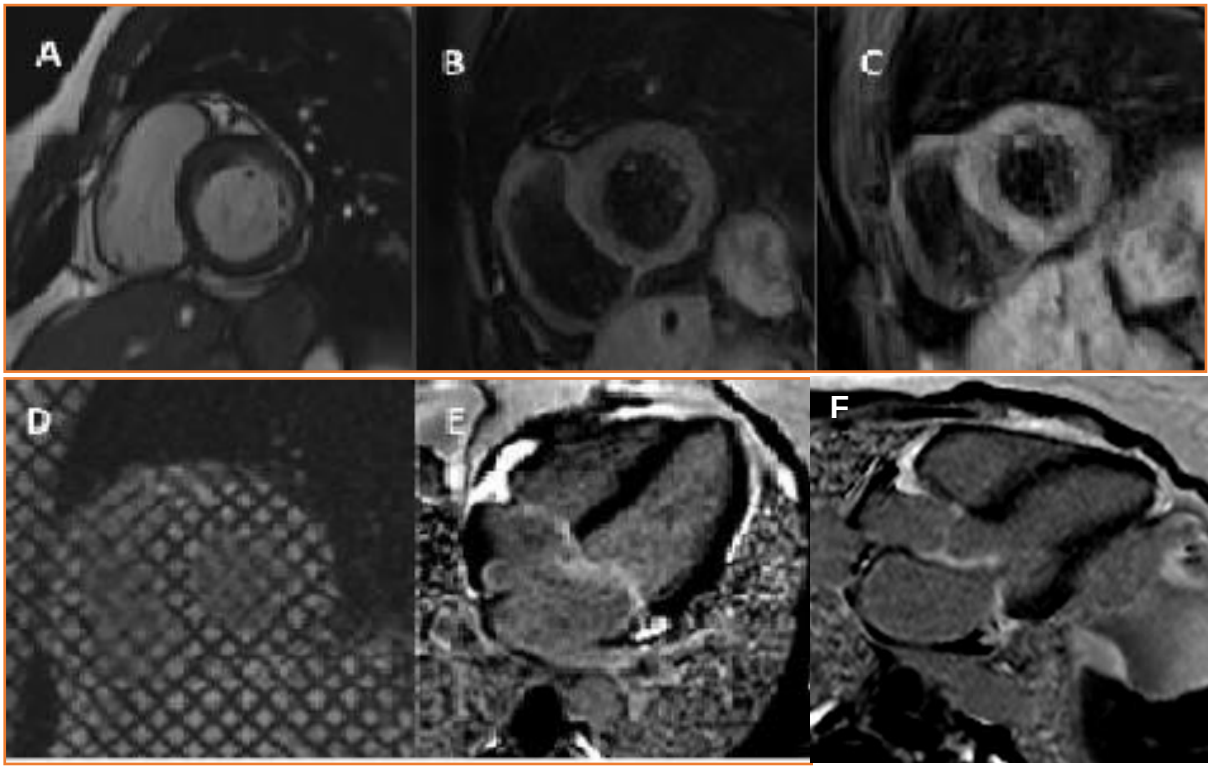

Figure 2.4: CMR in subject with heart block and acute myocarditis confirmed to be due to acute rheumatic fever

A. SSFP Short axis (SA) cine showing normal LV and RV mass
B. T1-weighted image showing increased myocardial signal-intensity ratio;
C. T2-weighted imaging showing increased myocardial signal-intensity ratio (suggestive of myocardial oedema);
D. Ciné tagging SA imaging confirming impaired circumferential systolic- and diastolic strain rate;
E. Horizontal long-axis (four- chamber) LGE image showing no myocardial enhancement but striking enhancement of mitral and tricuspid valves;
F. Left ventricular outflow tract (LVOT view)
(Adopted from Samuels et al., 2017)

Edwards and colleagues conducted a cross-sectional CMR study on 35 patients (mean age 64 years), with asymptomatic moderate and severe primary degenerative mitral regurgitation, but impaired VO_2 max. The authors reported dilated LV volumes, normal LV systolic function with evidence of impaired longitudinal and circumferential strain. LGE was found in 30% of subjects as well as evidence of diffuse myocardial fibrosis from elevated ECV values. LGE pattern was predominantly diffuse, mid-wall and not consistent with coronary artery territory. The authors concluded that increased myocardial fibrosis, impaired myocardial strain and lowered exercise capacity are

characteristic of patients with moderate to severe mitral regurgitation (Edwards et al., 2014).

Shriki and colleagues reported an unfamiliar finding in 3 patients with RHD. Patient 1 was a 36-year-old female. CMR showed severe TRr, severe RV dilatation with globally diminished RV function. The patient had a prosthetic mitral valve which made it difficult to quantify MR and MS. LGE was extensive and patchy in the left and right atrial walls (Shriki et al., 2011). Patient 2 was a 68-year-old male. CMR revealed severely diminished LV systolic function, thickened mitral leaflets, moderate MS and MR. Similar to patient 1, LGE was present in the atrial walls as well as in the atrioventricular valves. The third patient was an 82-year-old male with significant bi-atrial dilatation on CMR, mild ventricular dilatation, severe MR and TRr and mild MS. LGE pattern was found to be patchy and extensive in both atrial walls (Shriki et al., 2011).

Meel and colleagues investigated the presence of fibrosis using LGE and biomarkers of collagen turnover in 22 patients with chronic rheumatic mitral regurgitation (CRMR) and found LGE in 18% of CRMR patients; none was observed in the controls. A mixed pattern of LGE of the LV myocardium was observed in RHD patients. These were transmural LGE in the lateral wall, transmural fibrosis of the inferior wall, patchy LGE in parts of the basal septum, mid-septum and basal inferior wall. One patient had sub-epicardial LGE. Coronary angiograms, done as part of their surgical work-up, were normal in both patients with transmural involvement (Meel et al., 2018). Both CMR and echocardiography revealed increased LV dimensions and LV mass in patients, however LV systolic function did not differ. Procollagen 1C peptide (PIP) and procollagen III N-terminal pro-peptide (PIIINP) were comparable between patients and controls, however, matrix metalloproteinase-1 (MMP-1) activity was elevated in RHD patients. The authors concluded that CRMR is distinguished by the prevalence of collagen degradation instead of increased synthesis and myocardial fibrosis (Meel et al., 2018).

Mutnuru et al., (2016) conducted a prospective longitudinal study on 50 patients over a period of 4 years, to define the role of CMR in the evaluation of RHD and to compare the role of CMR with transthoracic echocardiography in quantification of stenosis and volume regurgitation. These authors found a prevalence of mitral stenosis both as an isolated abnormality and in combination with other valvular lesions. CMR confirmed all

cases with significant valvular stenosis and regurgitations on echocardiography. Similarly, there was a strong correlation between the findings of the 2 modalities for ejection fraction (Mutnuru et al., 2016). The correlation coefficient was 0.98 for average mitral valve area and 0.92 for average aortic valve area which was indicative of a strong positive association between the results by echocardiography and CMR. The sensitivity and specificity for echocardiography was 98% and 100% respectively, compared to 90% and 50% for MRI in the diagnosis of valvular lesions (Mutnuru et al., 2016).

Ferreira et al., (2014) investigated the value of T1 mapping in sixty patients with suspected acute myocarditis. Coronary artery disease was excluded in all patients and 93% had a history of recent systemic viral or inflammatory illness. Results showed that patients had a remarkably lower LVEF compared to controls as well as increased global T2 signal intensity ratio, suggestive of myocardial oedema. The LGE pattern was mainly subepicardial (96%) and mid-wall (84%), involving the lateral wall (98%) and inferior wall (96%). This is typical for myocarditis. Patients were subdivided into 3 groups in order to ascertain the value of T1 mapping compared to conventional techniques in the detection of myocarditis. Group 1 consisted of patients with a positive finding of oedema plus LGE; group 2 had no oedema, but positive LGE and Group 3 had neither oedema nor LGE. All patient subgroups showed a remarkable increase in the extent of myocardial injury on T1-mapping, using a threshold of T1 ≥ 990 ms, compared to T2 and LGE imaging (Ferreira et al., 2014). Native T1 mapping was able to demonstrate typical non-ischaemic enhancement patterns in acute myocarditis, similar to LGE. T1 showed increased sensitivity in the detection of additional areas of myocardial involvement compared to T2 weighted and LGE imaging (Ferreira et al., 2014).

CHAPTER THREE
RESEARCH METHODOLOGY

3.1 Chapter introduction

This chapter provides a comprehensive discussion of the research methodology employed in this study. A variety of CMR sequences and techniques are described which are important to assess the structure and function of the heart and heart valves. Cardiac function is affected by valvular insufficiency which is characteristic and common in patients with RHD. Furthermore, both qualitative as well as quantitative methods, such as LGE and parametric mapping tools for the diagnosis of myocardial fibrosis will be discussed.

3.2 Aim

The primary aim of the study was to document the extent of myocardial fibrosis and dysfunction in patients with RHD.

3.3 Objectives

The objectives of this study were to:

3.3.1 assess the extent of valvular disease in subjects with RHD

3.3.2 assess LV function in subjects with RHD

3.3.3 assess strain abnormalities in RHD

3.3.4 assess focal and diffuse myocardial fibrosis in RHD

3.4 Study design

This research project employed a quantitative, prospective research design aimed at assessing the extent of myocardial fibrosis in subjects with chronic RHD. Subjects with chronic RHD that met inclusion criteria, between the ages of 18 and 70 years were enrolled over a 24-month period. Subjects were recruited by one of the research fellows, involved in the main study. The main study was focused on characterising the phenotypes of myocardial inflammation, fibrosis and subject-specific ventricular remodelling and mathematical remodelling of LV geometry in RHD. Subjects were recruited from the Cardiac Clinic at an academic hospital in the Cape Metropole, Western Cape Province.

All research subjects underwent CMR, which included a variety of scanning sequences discussed in this chapter. Subjects had to be willing to undergo CMR on a voluntary

basis on a 3T MRI scanner located at an academic hospital. A detailed explanation of the procedure was given to all subjects in order to obtain fully informed signed consent, discussed later in this chapter.

3.5 Study population

This study consisted of 44 adults of both sexes and multiple ethnicities, with a confirmed history of chronic RHD. Thirty age-, sex-, and ethnicity matched, healthy controls were recruited for comparison. Controls were recruited by word of mouth. Controls with co-morbidities such as hypertension, diabetes and renal impairment were excluded. This study formed part of a larger cohort, which aimed to recruit approximately 200 subjects. The study was conducted under the leadership of Professor Ntobeko Ntusi, the Head of Medicine at an academic hospital. At writing up of this thesis, the main study was still in progress.

3.5.1 Inclusion criteria

The following criteria was applied to recruit subjects for this study:

- Subjects with chronic RHD, confirmed with echocardiography
- Adults between 18 and 70 years, willing to participate voluntarily
- Subjects of sound mind and able to provide informed consent

3.5.2 Exclusion criteria

The following exclusion criteria was applied:

- Pregnant females
- Subjects with contraindication(s) to MRI, such as:
    - claustrophobia
    - metallic or electronic implants in their bodies. Ferromagnetic materials, such as iron and stainless steel are contraindicated in the MRI scanner as these devices may result in excessive heating during the scan, which may cause damage to the surrounding body tissue.
    - The magnetic field of the MRI scanner can damage electronic devices such as pacemakers and cochlear implants. Therefore, subjects with these types of implants were excluded.
    - Subjects with prosthetic heart valves
- Subjects with renal impairment for example an eGFR < 30 ml/min
- Subjects under 18 years of age

- Subjects that were considered a vulnerable population such as psychiatric, or frail individuals or inmates who met the inclusion criteria above
- Critically ill subjects referred from an intensive care unit

3.5.3 Recruitment and enrolment

The study population included subjects with a chronic history of RHD who met the inclusion criteria. Recruitment was done by a research fellow doing recruitment for the main study. Recruitment was done under the guidance of the doctors and nurses employed at the Cardiac Clinic, at an academic hospital. As part of the recruitment process, subjects were assessed to make sure that they were fit enough to hold their breath during the scanning procedure and were able to lie in the supine position for the entire duration of the scan. The CMR procedure was explained to the subject who then signed the MRI compatibility checklist **(Appendix E)** once he/she agreed to participate. An information leaflet **(Appendix D)** was handed to each subject for perusal and further reference. Thirty matched healthy volunteers were recruited by word of mouth for comparison.

3.5.4 Sampling size strategy

Based on echocardiographic screening, the prevalence of RHD in Cape Town communities is reported as 20/1000 in school children (Zühlke et al., 2015). Based on the pilot data and data generated by the clinical service at the research site, we estimated that the difference in T1 values is normally distributed with a standard deviation of 29. If the true difference in the tissue characteristics between RHD subjects and controls is 0.5, the researchers would need to study 44 subjects to be able to reject the null hypothesis that the difference is zero with a probability (power) of 0.99. The type I error probability associated with this test of the null hypothesis was 0.01. Based on our subject numbers and access to the MRI scanner, the provisional sample size for this project was 44 RHD subjects, and study population increased to 50 to account for subject loss.

3.6 CMR imaging acquisition

All eligible subjects were scanned on a 3T Siemens Magnetom Skyra scanner, manufactured in Erlangen, Germany. Scans were performed by radiographers, competent in CMR imaging, at a research imaging centre based at an academic hospital.

3.6.1 Subject preparation outside the scanner room

Subjects were asked to remove all clothing and changed into a cotton gown to prevent overheating during scanning. All accessories such as jewellery, hairclips and personal belongings such as wallets with bank cards were removed and locked away. The MRI compatibility checklist was completed and signed by both subject and radiographer. An intravenous cannula was placed in the median cubital fossa, by one of the clinicians from the Cardiac Clinic, to facilitate the administration of contrast media. All subjects were asked to empty their bladder before commencement of the scan to minimise disruption during image acquisition.

3.6.2 Subject preparation inside the scanner room

All subjects were scanned in the head-first, supine position. To ensure comfort, a pillow was placed under the head and a wedge under the knees of all subjects. In order to ensure privacy, subjects were covered with a sheet or light blanket. A squeeze ball was handed to all subjects which could be used as an alarm in case they required any assistance during the procedure. The subject's skin, over the thorax, was cleaned with Nu-prep® exfoliating gel for the placement of the ECG electrodes. Males with chest hair were asked to shave the anterior thorax prior to the procedure. The breath-hold instructions were practiced, with all subjects to ensure compliance with arrested expiration during the image acquisition. The subject was positioned in such a way that the top of the thorax was positioned at the level of the first element of the spine coil. An 18-channel body array coil was placed over the chest with the heart in the centre of the coil. MRI compatible headphones were placed over their ears to reduce the acoustic noise of the scanner and to ensure that subjects could hear the breathing instructions during the scan.

3.7 CMR protocol

3.7.1 Localising and pilot sequences

The scanning protocol included the following sequences:

- Localisers in the axial, coronal and sagittal planes to determine the subject's position inside the gantry.
- Half-Fourier-Acquired Single-shot Turbo spin Echo (HASTE)
  - Axial views: from the neck vessels to the inferior border of the right ventricle.

- Coronal views: planned from the posterior border of the descending aorta to the anterior border of the right ventricle.

The above sequences were obtained to get an overview of the anatomical structures of the thorax in relation to the heart and to assess for incidental extra-cardiac pathology. To examine the heart in its entirety, the usual orthogonal planes of the body, namely axial, coronal and sagittal cannot be employed. Instead, the complex oblique planes of the heart were used for image acquisition. The following section provides a detailed description of how these complex planes were achieved.

Pilot sequences were done in the 2- chamber, 4- chamber and short axis planes to place the heart in the isocentre of the magnetic field. The 2-chamber pilot view was obtained by using the transverse or axial HASTE sequence as a reference. Planning was done parallel to the intraventricular septum, bisecting the apex of the left ventricle, mitral valve and left atrium (Fig. 3.1).

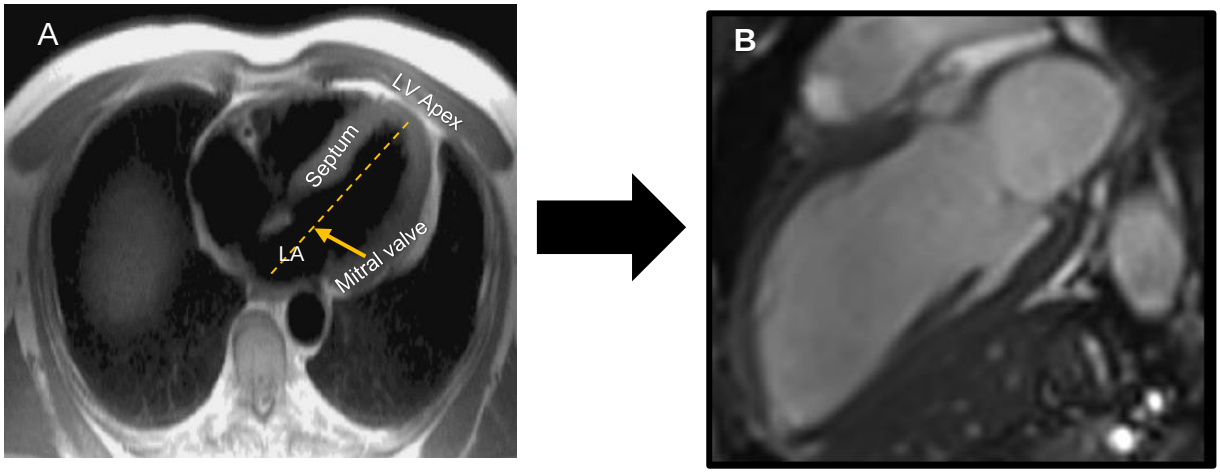

A: Axial HASTE view **B: 2 Chamber view**

Figure 3.1: Axial HASTE view (A) showing how to plan 2 chamber view (B)
(Permission to use images was granted by the subject)

To obtain the 4-chamber pilot, the sequence was planned on the 2-chamber view. Planning line bisected the apex of the LV, mitral valve and LA (Fig. 3.2).

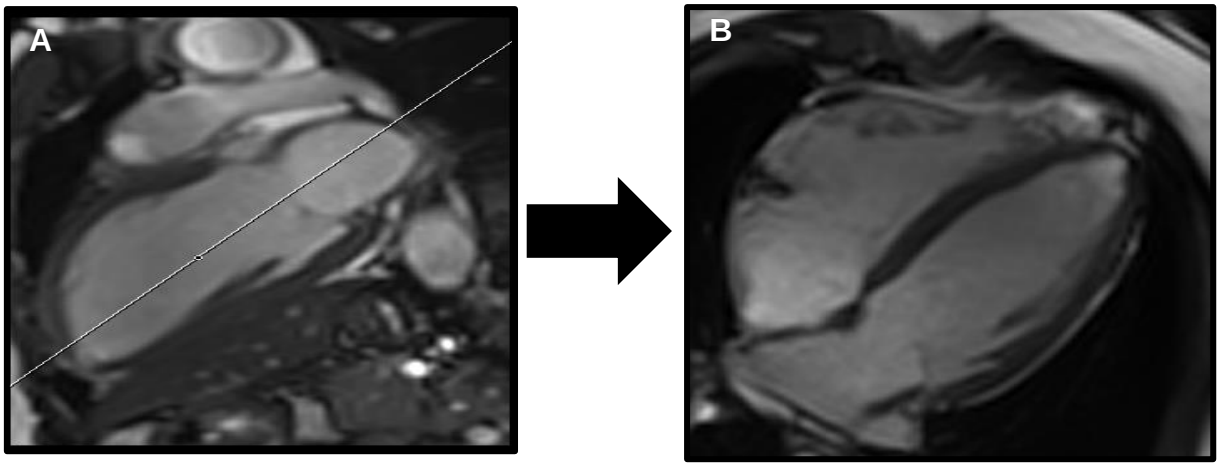

A: 2-chamber view **B: 4-chamber view**

Figure 3.2: Showing the planning of the 4-chamber view
(Permission to use images was granted by the subject)

The short axis (SA) pilot was planned, using both the 2- and 4-chamber views. The SA view was planned parallel to the base of the LA and LV (Fig. 3.3).

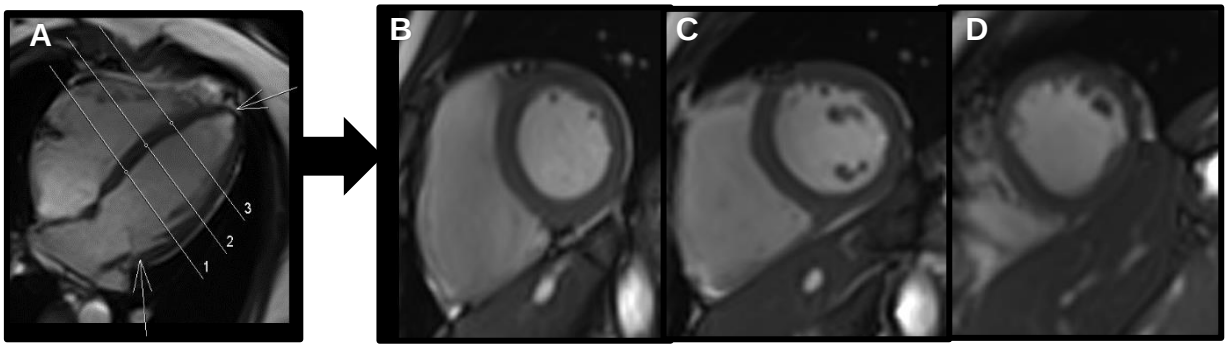

A: SA plan on 4-chamber view **B: SA base** **C: SA mid ventricle** **D: SA apex**

Figure 3.3: Showing the planning of the SA stack on 4-chamber view
(Permission to use images was granted by the subject)

3.7.2 Cine imaging

Cine images are short motion images used to demonstrate the motion of the heart throughout the entire cardiac cycle. All cine images were acquired by using a segmented approach. The cardiac cycle, which starts with the R wave of the ECG and ends with the succeeding R wave, was divided into several segments. The number of segments were determined by the heart rate and ranged between 10 and 20 segments. Cine images were created by collecting information over several heart beats resulting in a final sequence which consisted of several frames that can be viewed as a movie. A SSFP sequence was used for functional analysis of the heart.

The sequence parameters were as follows: TR = 43.08 ms, TE = 1.61 ms, flip angle (FA) = 40°, matrix size = 149 x 208, Bandwidth (BW) = 962 Hz/Px, slice thickness = 6 mm and 25 phases. The sequence was acquired over 9 heartbeats per slice.

For LV and RV function, cine images were acquired in the following orientations as displayed in Table 3.1 and Table 3.2.

Table 3.1: Cine images for left ventricular function

Orientation	Purpose
4-chamber cine sequence	For the assessment of the ventricles and atria To assess mitral and tricuspid valves for stenosis and regurgitation
2-chamber cine sequence	For the assessment of the left ventricle, atrium and mitral valve
Left ventricular outflow tract (LVOT)	To assess the aortic valve for stenosis and regurgitation
Coronal LVOT	To assess aortic valve and proximal aortic disease
Short axis (SA) stack – from the base to the apex of the heart	For the assessment of stroke volumes and to quantify LV and RV ejection fractions

Table 3.2: Cine images for right ventricular function

Orientation	Purpose
RV 2-chamber cine sequence	For the assessment of the right ventricle, atrium and tricuspid valve
RV 3-chamber cine sequence	To assess the inflow from the superior vena cava (SVC) into the right atrium and right ventricle
Right ventricular outflow tract (RVOT)	To assess outflow from the RV into the infundibulum and through the pulmonary valve
Coronal RVOT	For RV outflow and assessment of the main pulmonary artery

3.7.3 Cine tagging imaging

Cine tagged images were obtained in the SA plane at the base, middle and apex as well as the 4-chamber plane for the assessment of myocardial strain (Fig. 3.4).

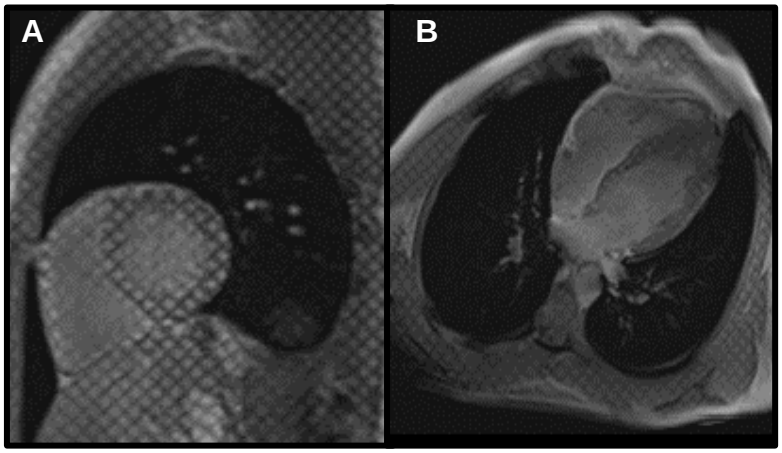

A: SA Tagging mid ventricle **B: 4-Chamber**

Figure 3.4: Showing gridlines in the myocardium on short axis (A) and 4-chamber cine tagging images

(Permission to use images was granted by the subject)

3.7.4 T2 Short-Tau-inversion-recovery imaging

The short Tau inversion-recovery (STIR) technique allows suppression of the pericardial fat and moving blood within the chambers, which will emphasise inflammatory changes in the myocardium, due to excess water content in inflamed

tissues. Sequences were acquired in the short axis plane of the heart at the base, middle and apex of the heart. For this approach, the skeletal muscle signal intensity was used as a reference to determine whether myocardial signal was abnormally high (Fig. 3.5).

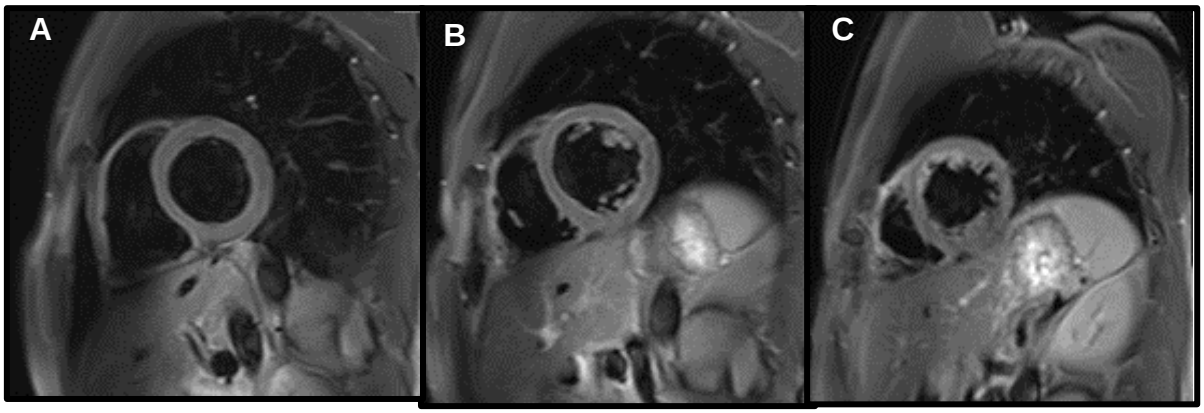

A: SA base **B: SA mid ventricle** **C: SA apex**

Figure 3.5: STIR images at the base, mid ventricle and apex
(Permission to use the images was granted by the subject)

3.7.5 T1 mapping

For T1 mapping, SA scans were obtained at the base, middle and apex of the left ventricle, over 11 heartbeats, using a 5:3:3 scheme, for a quantitative assessment of myocardial fibrosis. The imaging parameters employed were as follows: TR = 280.56 ms, TE = 1.12 ms, FA = 35°, acquisition matrix = 144 × 256, pixel size = 1.41 × 1.41 mm^2, slice thickness = 8 mm. The result is a colour or pixel-wise map with each pixel representing the measured T1 value of myocardial tissue (Fig. 3.6).

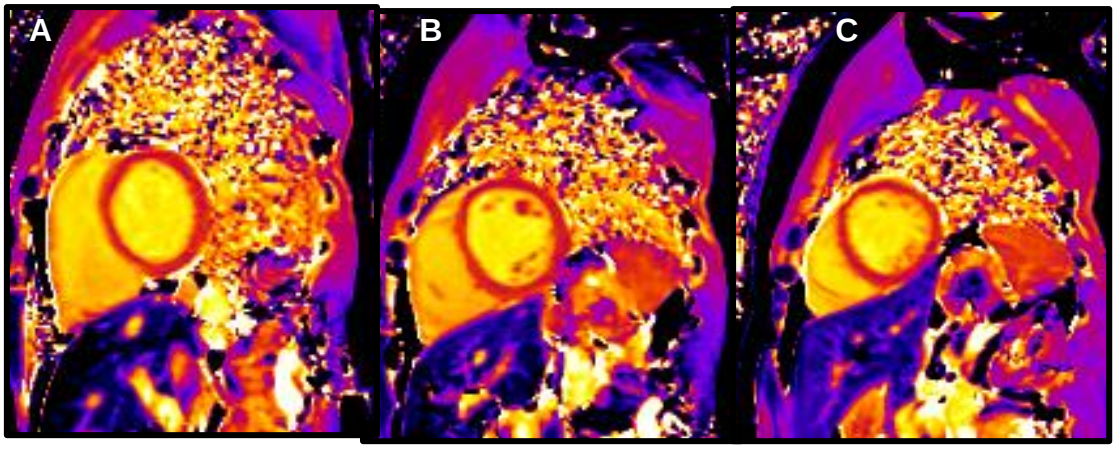

A: SA base **B: SA mid ventricle** **C: SA apex**

Figure 3.6: Short axis T1 Pre-contrast maps at the base, middle and apex of the left ventricle

(Permission to use the images was granted by the subject)

3.7.6 T2 Mapping

T2 maps employed were acquired in the same orientation as the T1 native maps and were used for the assessment of myocardial oedema. Imaging parameters were as follows: TR = 207.39 ms, TE = 1.3 ms, FA = 12º, acquisition matrix = 116 x 192, voxel size = 1.9 x 1.9 x 8.0 mm, slice thickness = 8 mm (Fig. 3.7).

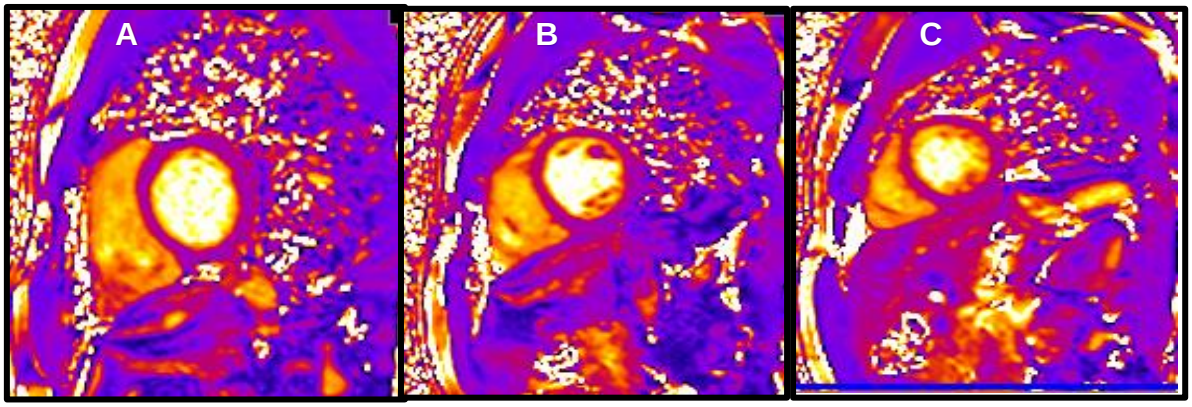

A: SA base **B: SA mid ventricle** **C: SA apex**

Figure 3.7: Short axis T2 Maps at base, mid ventricle and apex

(Permission to use the images was granted by the patient)

3.7.7 Post-contrast T1 mapping

Post-contrast T1 maps were obtained in the SA orientation at the base, middle and apex of the LV myocardium. Sequence parameters were as follows: TR = 360.56 ms, TE = 1.12 ms, FA = 35º, acquisition matrix = 144 x 256 mm, voxel size = 1.4 x 1.4 x 8.0 mm, slice thickness = 8 mm (Fig. 3.8).

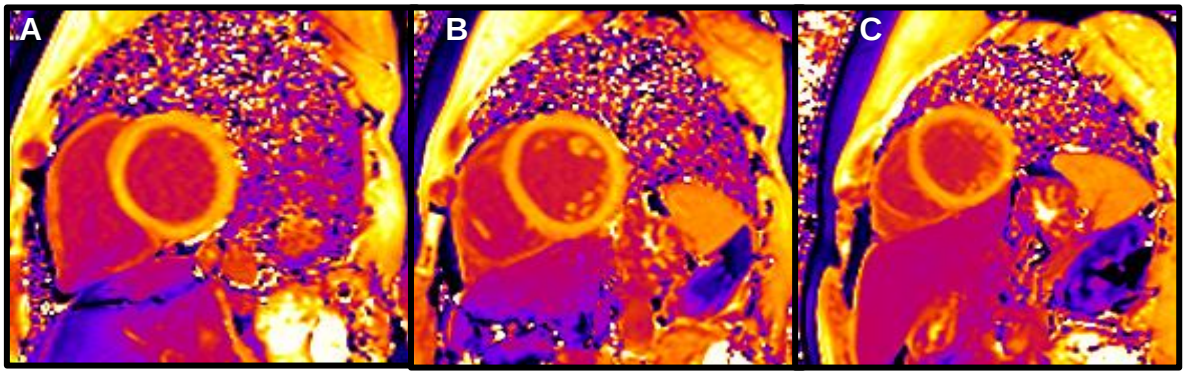

A: SA base **B: SA mid ventricle** **C: SA apex**

Figure 3.8: Short axis T1 Maps post-contrast administration

(Permission to use the images was granted by the subject)

3.7.8 Late gadolinium enhancement

An injection of gadopentetate dimeglumine (Magnevist) at 0.2mg/kg of body weight was administered by hand into the median cubital vein, followed by a 10-15 ml saline flush. LGE images were acquired using a T1-weighted phase-sensitive-inversion-recovery (PSIR) sequence. The imaging parameters were as follows: TR = 750, TE = 1.96 ms, FA = 20°, acquisition matrix = 140 x 256, slice thickness = 8 mm. Inversion time varied from subject to subject and was determined based on an inversion time (TI) scout which was acquired in the SA plane at the mid-level after 6 minutes following the contrast injection. Several slices were acquired with a single breath hold and inversion times ranging from 300 ms to 450 ms. The slice with optimal nulling of the myocardium (black myocardium and grey blood pool) was chosen to set the TI for the LGE images. The latter were acquired in the SA plane, from the base to the apex, 4-chamber, 2-chamber and LVOT planes. Inversion times ranged from 300 - 450 ms.

3.8 Data handling

All subjects were issued with a unique study identification code. Names of subjects and controls with their corresponding study codes were recorded in an Excel spreadsheet only accessible to the researcher. This was done to communicate incidental findings in controls as well as to ensure prompt follow-up for subjects. Images were transferred to the research imaging centre server in an anonymised folder called RHD. The researcher was provided with a unique password which allowed access to said folder. Images are stored on the server indefinitely. These images were also transferred to an external hard drive as a back-up measure. The external hard drive was kept in a locked drawer.

3.9 Image analysis

Data was imported from the server into CVI42 (Circle Cardiovascular Imaging, Calgary, Alberta) software for analysis. Images were analysed by an experienced reader, blinded to the echocardiographic results. The image analysis for LVEF as well as RV ejection fraction (RVEF) was performed using CVI42 software. The SA stack was used to plan manual contouring of the epicardial and endocardial borders of the LV in end-diastole (LVEDV) and end-systole (LVESV) and used to calculate the stroke volume (SV) and LVEF. SV was calculated as the difference between the EDV and the ESV. Therefore: SV = EDV – ESV. The formula used to calculate EF is as follows: EF = SV/EDV. The epicardial contours were traced in the end-diastolic and end-systolic

phases for calculation of the ventricular mass. Myocardial mass was determined by subtracting endocardial volume from the epicardial volume and multiplying by the density of the myocardium:

$m_{myo} = \eta_{myo} \times (ESV – EDV)$ (Suinesiaputra et al., 2015).

All values were normalised (indexed) by dividing the absolute value by body surface area (BSA).

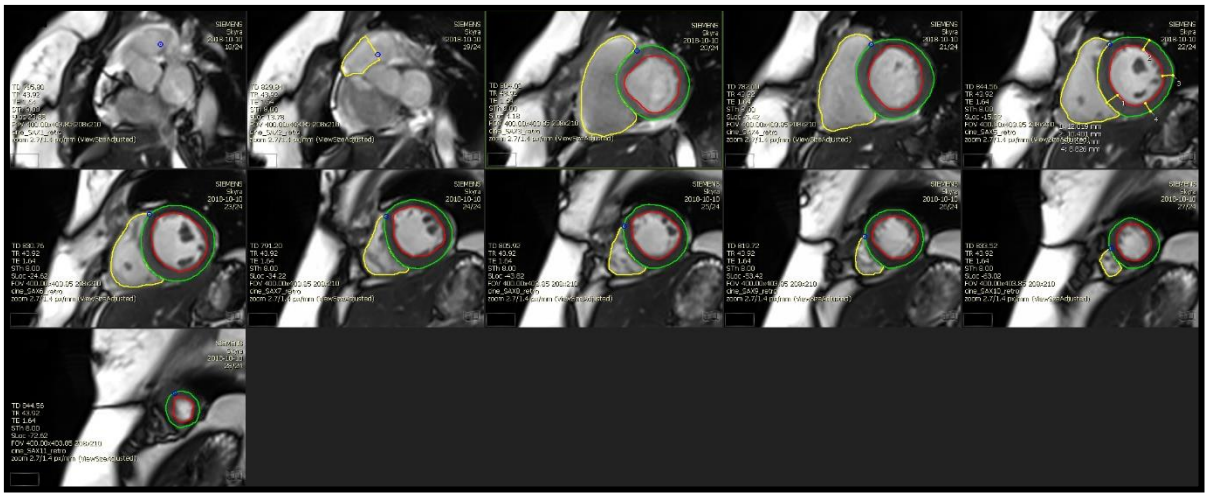

Figure 3.9: Contouring of the SA stack in end-diastole
(Permission to use the images was granted by the subject)

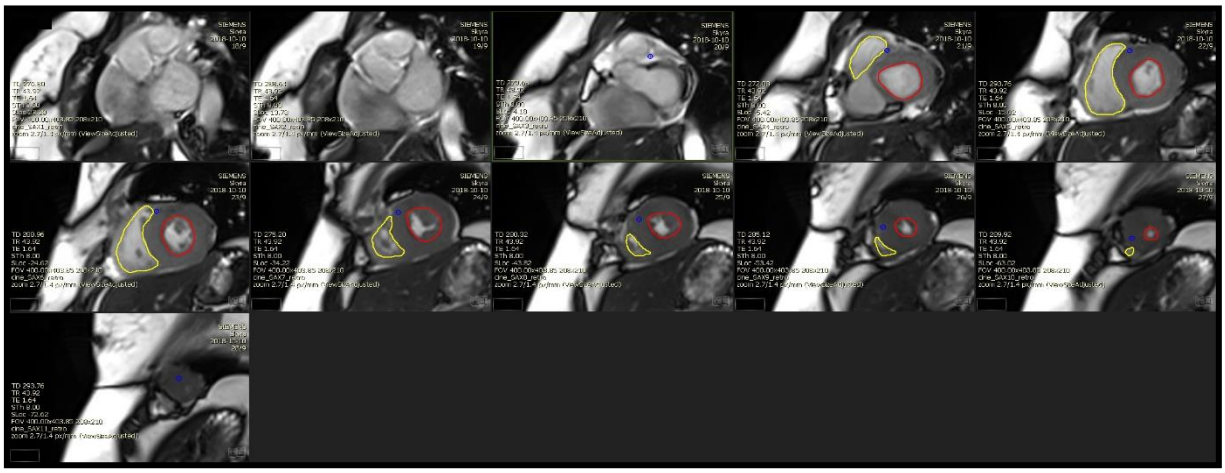

Figure 3.10: Contouring of the SA stack in end-systole
(Permission to use the images was granted by the subject)

3.9.1 T2-weighted short Tau inversion-recovery images

Quantitative analysis of STIR images was performed by drawing a region-of-interest (ROI) in the LV myocardium and comparing the signal intensity to that of adjacent skeletal muscle in the same slice. A signal intensity ratio > 1.9 supported the evidence of myocardial oedema. Drawing a ROI in the myocardium and remote skeletal muscle to determine the presence of myocardial oedema. The ratio should be < 1.9 - 1 in normal myocardium. (Fig. 3.11) (Ntusi et al., 2015).

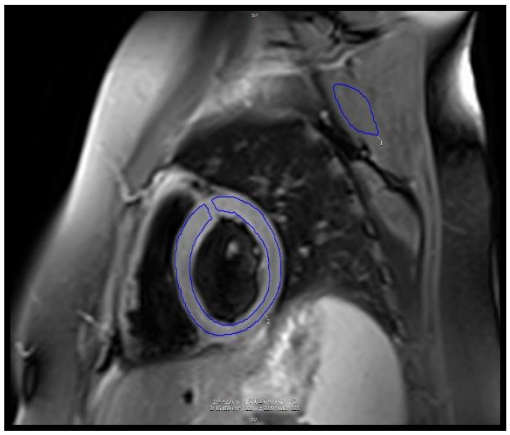

Figure 3.11: T2 STIR Short axis view
(Permission to use the images was granted by the subject)

3.9.2 T1-weighted images

Drawing a ROI in the myocardium and skeletal muscle (Fig. 3.12) to determine the presence of myocardial fibrosis. The signal intensity ratio should be < 1.9 - 1 in normal myocardium. Increased signal intensity ratio on T1 was considered an indication of myocardial fibrosis (Ntusi et al., 2015).

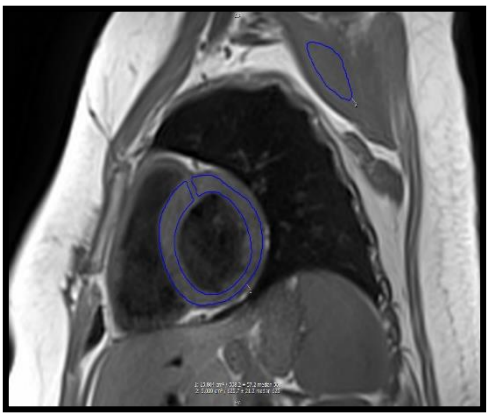

Figure 3.12: T1 weighted Short axis view

(Permission to use the images was granted by the subject)

Drawing a ROI in the myocardium on SA base, middle and apical views of the native T1 maps to determine T1 values to quantify myocardial fibrosis (Fig. 3.13).

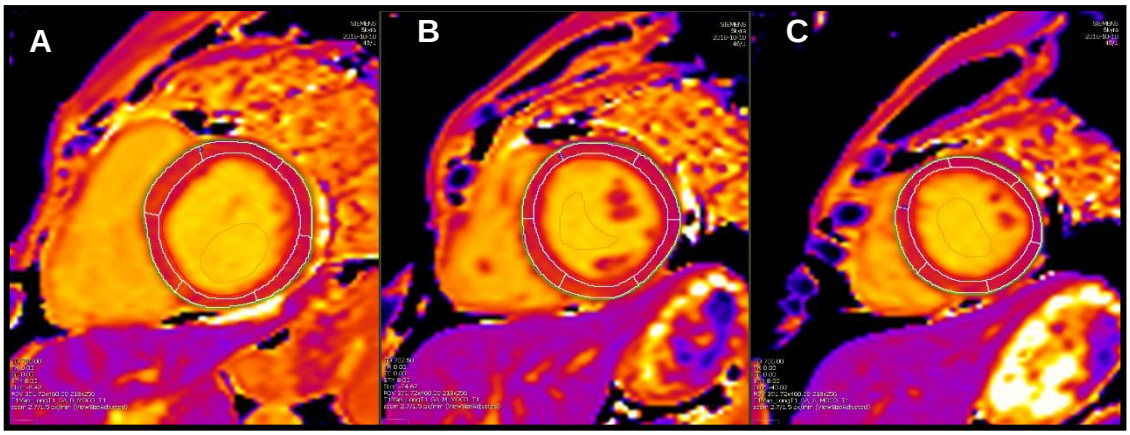

A: SA base **B: SA mid ventricle** **C: SA apex**

Figure 3.13: Short axis native T1 maps at the base, mid and apex

(Permission to use the images was granted by the subject)

Drawing a ROI in the myocardium on SA base, middle and apical views of the T2 maps to determine T2 values to quantify myocardial oedema (Fig. 3.14).

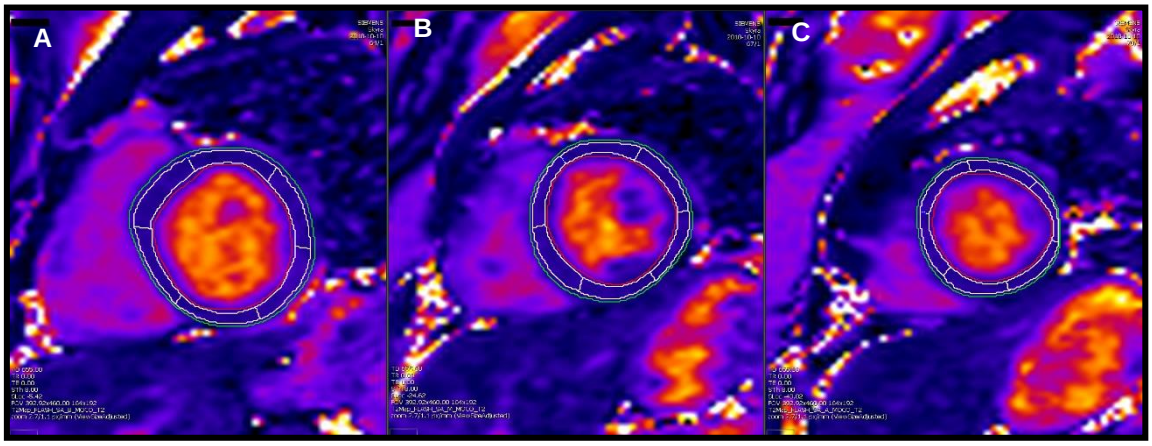

A: SA base **B: SA mid ventricle** **C: SA apex**

Figure 3.14: Short axis T2 maps at the base, mid and apex

(Permission to use the images was granted by the subject)

3.10 Statistical considerations

The Shapiro-Wilks test was used to test the normality of data. Normally distributed data were presented as mean ± standard deviation (SD) or, where results were highly skewed, as median (interquartile range). Discrete data were presented as numbers (percentages). For the comparison of discrete data, the Chi-square test was utilised, where appropriate. Mann-Whitney U test was used to compare not-normally distributed data. Pearson "R" and Spearman "R_S" coefficients were used to assess bivariate correlations, as appropriate. Determinants of myocardial inflammation, fibrosis and deformational characteristics was established by performing linear regression analysis. All statistical tests were two-tailed, with p-values of less than 0.05 considered statistically significant. All analysis was performed using Statistical Package for the Social Sciences (SPSS) version 25 (IBM, Armonk, New York, USA).

3.11 Ethical considerations

Ethics approval for this study was granted by the Research Ethics Committee of the Faculty of Health and Wellness Sciences at the Cape Peninsula University of Technology (CPUT) ***(CPUT/HW-REC 2017/H23)*** **(Appendix A)** as well as the Human Research Ethics Committee of the Faculty of Health Sciences of the University of Cape Town (UCT) **(Appendix B).** Site approval to conduct the study was also obtained from the Director of the research imaging centre **(Appendix C).**

The ethical standards upheld during the study were in accordance with the principles of the Helsinki Declaration in the following manner:

- Research was only conducted on subjects (patients and controls) who could provide informed consent. The researcher explained the procedure to subjects and a patient information leaflet **(Appendix D)** was handed to each subject. The patient information leaflet provided adequate information regarding the aims and methods of the research.
- All subjects were informed that they had the right to withdraw from the study at any time without being penalised (WMA, 2013).

The ethical guidelines of the Health Professions Council of South Africa (HPCSA) require that healthcare practitioners ensure that their research participants have a comprehensive understanding of the procedure that they are volunteering to partake in. Healthcare practitioners should explain what the study entails, the way it will be

executed, and the risks associated with it (HPCSA, 2008). Before commencement, the MRI procedure was explained, by the researcher, to each subject in their preferred language.

Subject participation was strictly voluntary, and subjects were not coerced to partake in the study by offering them any gifts. The Helsinki Declaration also emphasises the inherent risk and burden involved in medical research in human subjects. Research can only be conducted if it is preceded by a risk and burden assessment. Furthermore, it is imperative that the benefits in undertaking said research, outweigh the risks (WMA, 2013). The risks involved when undergoing MRI are minimal, provided one adheres to the safety precautions when preparing subjects or escorts. To minimise these risks, a checklist was completed **(Appendix E)** by the researcher to ensure that subjects did not have any metal implants that could be affected by, or that could affect the magnetic field. Since it is natural for subjects to experience heating during MR scanning, subjects were asked to remove all clothing that could potentially absorb heat during scanning and in view of this, all research subjects were changed into a cotton gown. Subjects who experienced discomfort during the procedure were attended to by the researcher and the required treatment was conducted based on the nature of their complaint. In order to maintain confidentiality, all subjects were assigned a unique study number, for example RHD_01_PS. All documents such as consent forms, patient compatibility checklists were filed and kept in a locked drawer to which only the researcher had access.

CHAPTER FOUR
RESEARCH RESULTS

4.1 Subject recruitment

Fifty RHD subjects were recruited of which 48 were scanned; 2 withdrew by way of non-attendance. Of the 48 subjects scanned, 3 had incomplete scans due to difficulty with breath-holds and claustrophobia. One subject had findings consistent with a diagnosis of dilated cardiomyopathy and was therefore excluded from the analysis. Thirty healthy controls were scanned for comparison.

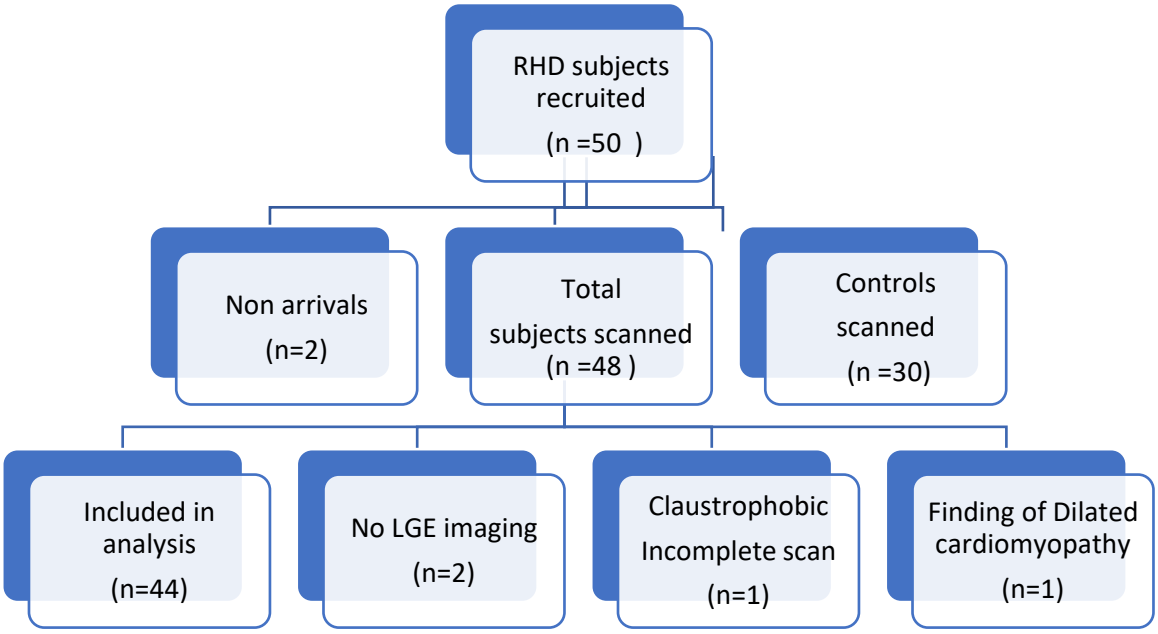

Figure 4.1: Flow diagram for recruitment of subjects for data analysis

4.2 Baseline characteristics

Table 4.1 outlines the baseline characteristics in RHD subjects and controls. Of 44 RHD subjects in the study, 63.6% were female and 36.4% male, with (47% male and 53% female) in the control group. The mean age of the study population was 42.84 ± 13.84 years and 38.87 ± 12.31 years in the control group. There were no significant differences when comparing age, height, weight, body mass index (BMI) and body surface area (BSA) between RHD subjects and controls. Just over half (52.3%) of subjects with RHD reported symptoms of effort intolerance (NYHA Class II 25%; NYHA Class III 27.3%). AF, secondary to RHD, was noted in 27.3% of patients. Hypertension

(34%) and smoking (16%) were the most commonly encountered co-morbidities in the RHD group. There were no reported symptoms or co-morbidities in the control group.

Table 4.1: Demographics and co-morbidities of subjects

	Subjects (n=44)	***Controls (n=30)***	***P values***
Age, years	42.84 ± 13.84	38.87 ± 12.31	0.21
Sex Female, n (%)	28 (63.63)	16 (53.33)	-
Ethnicity n (%) Black Mixed race	 19 (40.9) 26 (59.1)	 14 (46.6) 16 (53.4)	 - -
Heart rate, bpm	83.77 ± 28.05	72.57 ± 15.98	0.05
Height, m	1.64 ± 0.09	1.66 ± 0.09	0.53
Weight, kg	77.10 ± 21.83	76.90 ± 19.37	0.96
BMI, kg/m^2	28.31 ± 7.34	27.66 ± 5.65	0.68
BSA, m^2	1.85 ± 0.29	1.86 ± 0.27	0.84
NYHA, n (%) NYHA I NYHA II NYHA III NYHA IV	 21 (47.7) 11 (25) 12 (27.3) 0 (0)	 30 (100) - - -	 - - - -
AF, n (%)	12 (27.3)	-	-
Comorbidities			
Hypertension, n (%)	15 (34)	-	-
Dyslipidaemia, n (%)	1 (0.03)	-	-
Obesity, n (%)	1 (0.03)	-	-
HIV, n (%)	2 (0.05)	-	-
Smoking, n (%)	7 (16)	-	-
Hyperthyroidism, n (%)	1 (0.3)	-	-
Anaemia	1 (0.03)	-	-
Diabetes	2 (0.05)	-	-
Gout	1 (0.03)	-	-

Continuous data are mean ± SD unless otherwise indicated.

Characteristics are presented as 95% confidence interval (CI).

Bpm, beats per minute; m, meter; kg, kilograms; BMI, body mass index; BSA, body surface area, AF, Atrial fibrillation; HIV, Human immunodeficiency virus.

4.3 Cardiovascular magnetic resonance findings

There were significant differences between RHD subjects and controls for all CMR volumetric and functional parameters (Table 4.2). Subjects showed an increased indexed LV end-diastolic, end-systolic, and stroke volumes compared to controls (all p values < 0.001). The LVEF was lower in subjects and below normal range compared to controls (44.0 ± 13.26 % versus 56.9 ± 5.19 %, p < 0001). There was significant left atrial dilatation in RHD subjects compared to controls (41.37 ± 11.84 mm versus 21.77 ± 3.13 mm, p < 0001). Increased indexed RV end-diastolic, end-systolic and stroke

volumes were found. RVEF was significantly lower in subjects and below normal range compared to controls (41.07 ± 16.19% versus 53.60 ± 7.46%, p = 0.001).

Table 4.2: Ventricular volumes, mass and function

	Subjects (n=44)	***Controls (n=30)***	***P-values***
LVEDV*i*, ml/m^2	104.08 ± 35.36	74.3 2± 14.12	<0.001
LVESV*i*, ml/m^2	55.34 ± 19.25	32.27 ± 8.36	<0.001
LVSV*i*, ml/m^2	45.83 ± 18.73	42.06 ± 7.48	<0.001
LVEF, %	44.03 ± 13.26	56.87 ± 5.19	<0.001
LVM*i*, ml/m^2	58.39 ± 29.55	50.02 ± 8.81	<0.138
LA diameter, mm	41.37 ± 11.84	21.77 ± 3.13	<0.001
RVEDV*i*, ml/m^2	78.43 ± 24.06	73.50 ± 13.48	0.31
RVESV*i*, ml/m^2	47.09 ± 21.63	34.45 ± 9.60	0.01
RVSV*i*, ml/m^2	33.12 ± 14.06	38.96 ± 7.34	0.04
RVEF, %	41.07 ± 16.19	53.6 0± 7.46	<0.001
RA diameter, mm	24.37 ± 9.57	22.33 ± 4.99	0.28

Continuous data are mean ± SD, unless otherwise indicated. Values are indexed to body surface area. LVEDVi, left ventricular end-diastolic volume index; LVESVi, left ventricular end-systolic volume index; LVSVi, left ventricular systolic volume index; LVEF, left ventricular ejection fraction; LVMi, left ventricular mass index; LA, Left atrium; RVEDVi right, ventricular end-diastolic volume index; RVESVi, right ventricular end-systolic volume index; RVSVi, right ventricular systolic volume index; RVEF, right ventricular ejection fraction; RA, right atrium

Both stenotic and regurgitant lesions were observed in the RHD subjects (Table 4.3), and no valvular lesions were observed in the control group. Of 44 subjects, 77.3% had mitral valve stenosis; 17.6% mild, 27% moderate and 36% severe. Aortic stenosis was present in 38.6% of subjects; 35.3% mild, 35.3% moderate and 29.4% severe. Only 1 (2%) had tricuspid stenosis. There were no stenotic pulmonary valves observed in any of the RHD subjects (Fig. 4.2).

Mitral regurgitation was observed in 95.4% subjects. The degree of mitral regurgitation was mostly severe (76.2%), with an associated mild (11.9%) and moderate (11.9%) mitral regurgitation. We observed thickening of both the anterior and posterior leaflets of the mitral valve in 37 (84%) subjects. Aortic regurgitation was seen in 59% of

subjects; 30.8% mild, 19.2% moderate and 50% severe. The aortic valve was thickened in 26 (59%) subjects, with calcification of the leaflets in 1 (2%). Although tricuspid stenosis was rare, regurgitation was seen in 75% of subjects; 21.2% mild, 45.5% moderate and 33.3% severe. The morphology of the tricuspid valves showed thickening in 15.9% of subjects. The pulmonary valve was least affected with 15.9% regurgitant lesions of which 57.1% were mild and 42.9% moderate (Fig. 4.3). Pulmonary valve thickening was observed in 5 (11.4%) of subjects.

Table 4.3: Valvular lesions

Valves	Stenosis			Regurgitation		
	Mild	Moderate	Severe	Mild	Moderate	Severe
Mitral, n (%)	6 (17.6)	12 (27)	16 (36)	5 (11.9)	5 (11.9)	32 (76.2)
Tricuspid, n (%)	0 (0)	1 (2)	0 (0)	7 (21.2)	15 (45.5)	11(33.3)
Pulmonary, n (%)	0 (0)	0 (0)	0 (0)	4 (57.1)	3 (42.9)	0 (0)
Aortic, n (%)	6 (35.3)	6 (35.3)	5 (29.4)	8 (30.8)	5 (19.2)	13 (50)

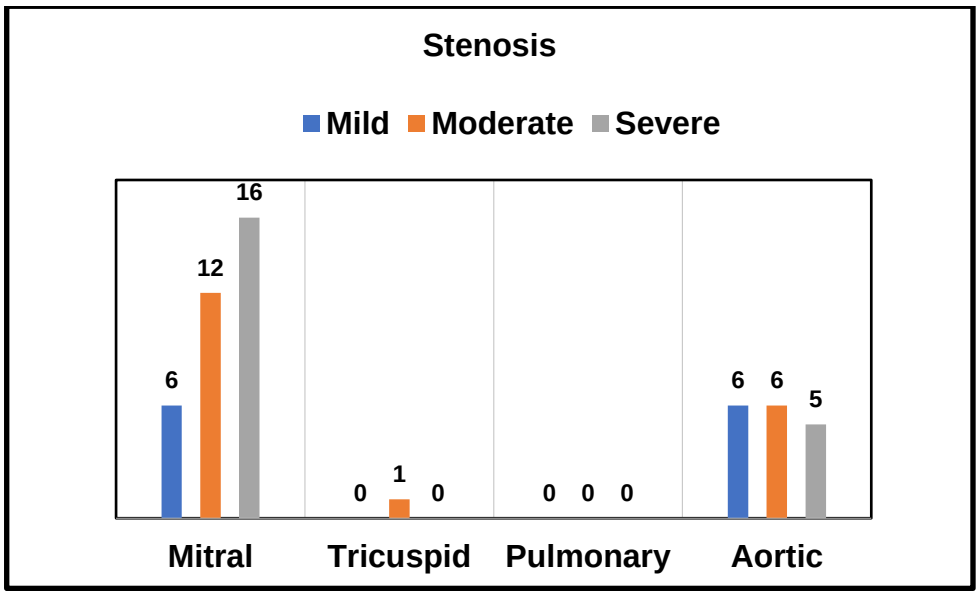

Figure 4.2: Illustration of valvular stenosis

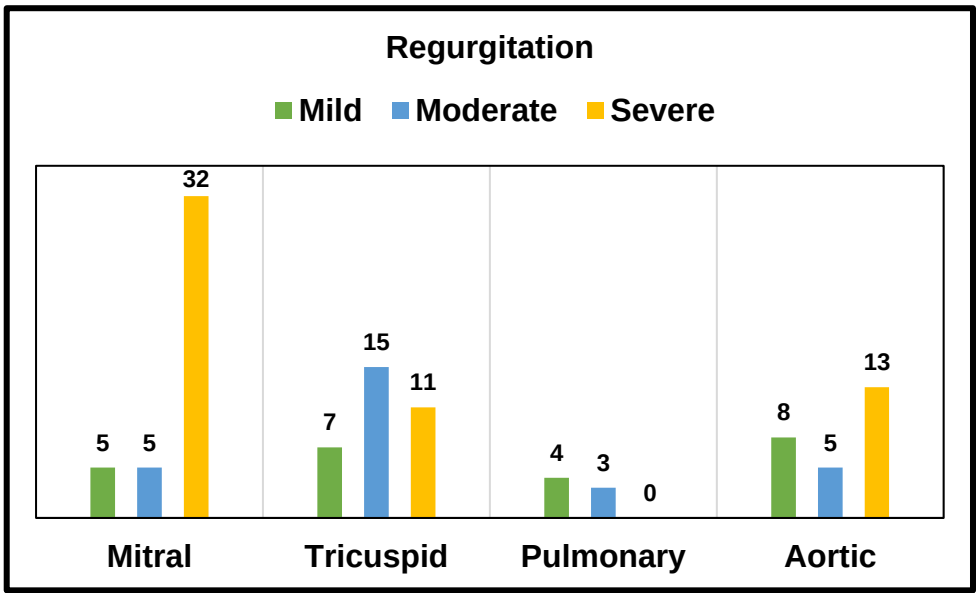

Figure 4.3: Illustration of valvular regurgitation

Most subjects had multiple valves involved with mixed valvular disease.

The figure below illustrates the percentage of left sided valvular lesions.

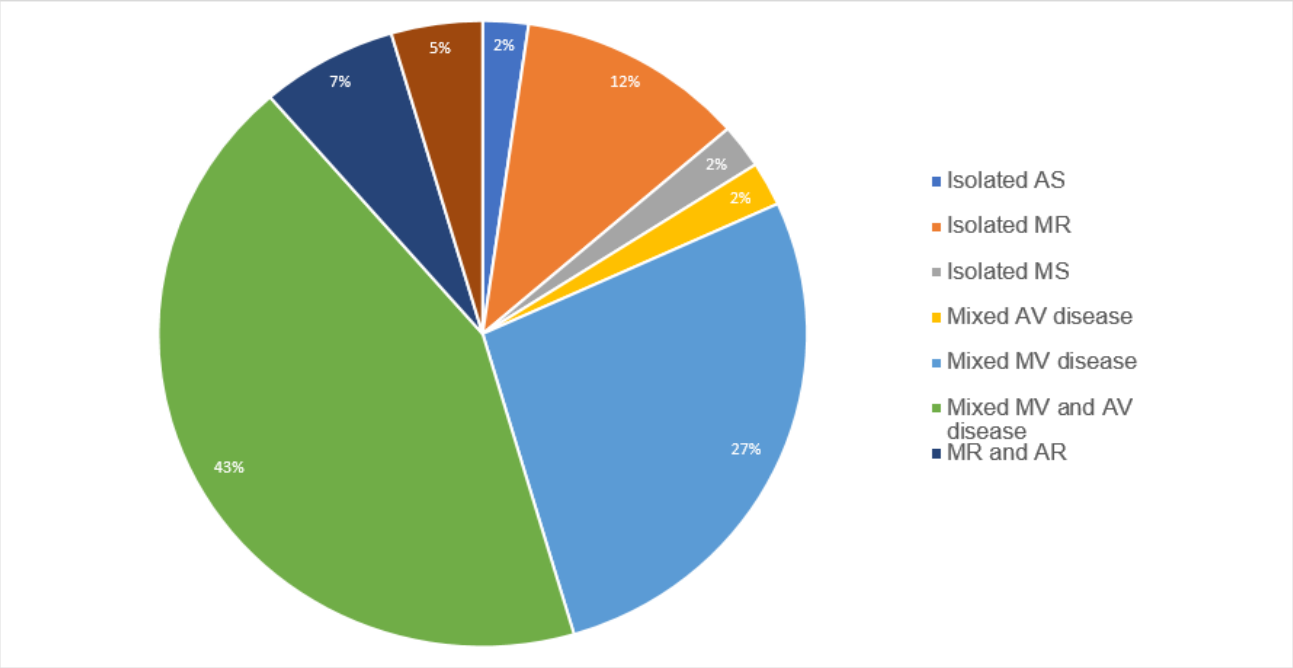

Figure 4.4: Pie chart illustrating valvular lesions on the left side of the heart
AS, aortic stenosis; MR, mitral regurgitation; MS, mitral stenosis; AV, aortic valve; MV, mitral valve; AR, aortic regurgitation

The boxplot below is an illustration of the relationship between valvular lesions and left ventricular ejection fraction.

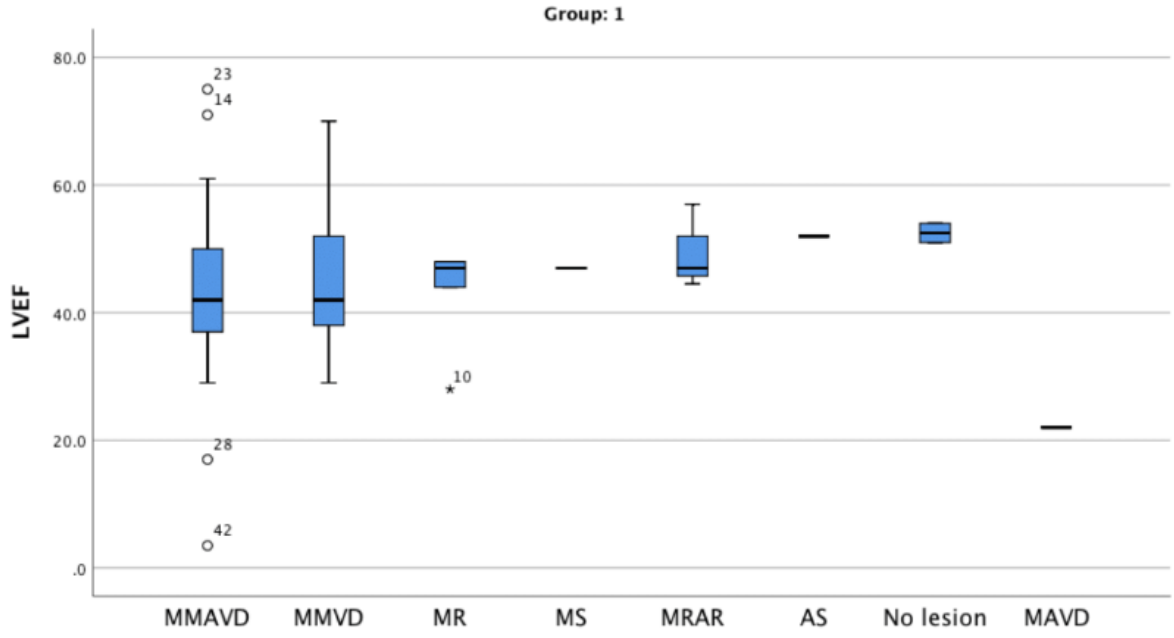

Figure 4.5: Boxplot illustrating the relationship between valvular lesions and left ventricular ejection fraction

MMAVD, mixed mitral and aortic valve disease; MMVD, mixed mitral valve disease; MR, mitral regurgitation; MS, mitral stenosis; MRAR, mitral regurgitation and aortic regurgitation; AS, aortic stenosis, MAVD, mixed aortic valve disease

LGE was evident in 100% of subjects with confirmed RHD, likely confirming disease chronicity and severity. LGE was circumferential in 79.5% of subjects, involving all segments. The specific patterns of enhancement were linear (26%), patchy (36%) and diffuse (38%). Enhancement of the mitral valve was present in 65.9% of subjects. Aortic valve enhancement was seen in 4.5% of subjects. LGE was observed in 20% of controls, in 5 a linear pattern of enhancement was observed and 1 showed patchy enhancement.

Figure 4.6 (below) illustrates the patterns of LGE in RDH subjects and controls. Researchers did not observe any features of structural heart disease in controls.

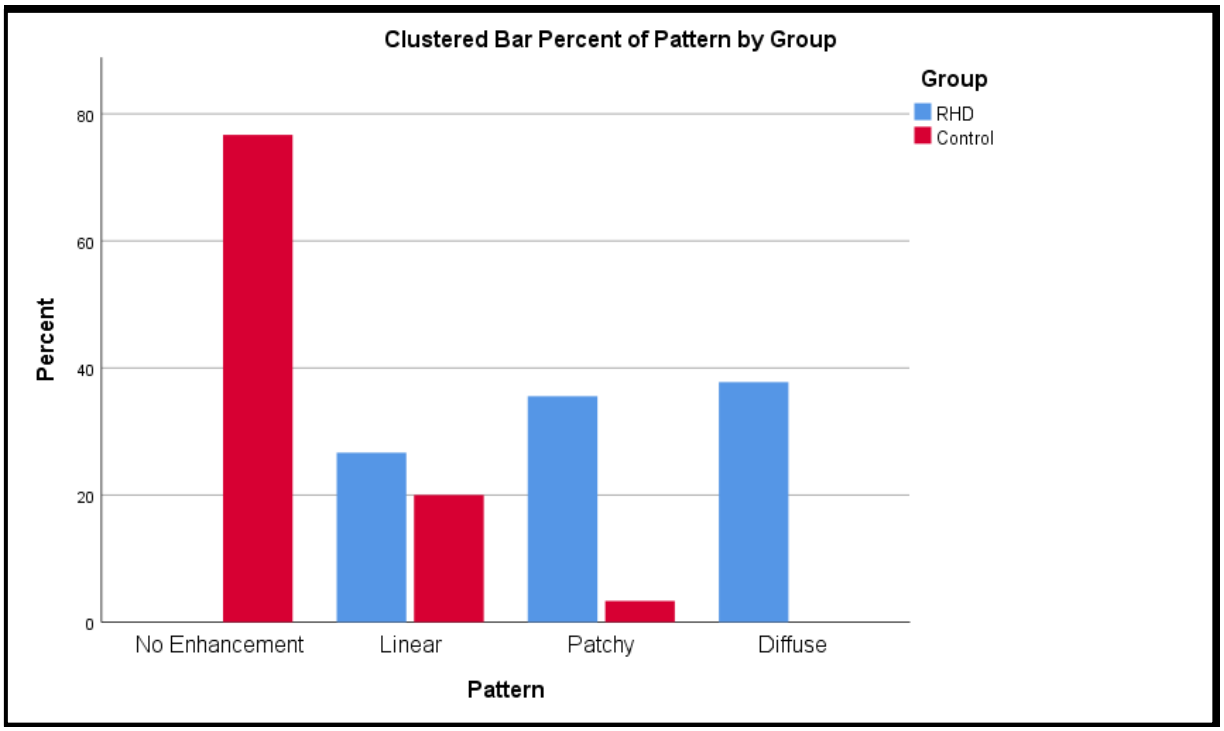

Figure 4.6: Bar graph illustrating patterns of late gadolinium enhancement in rheumatic heart disease subjects and controls

The figure below illustrates the patterns of LGE in relation to valvular lesions.

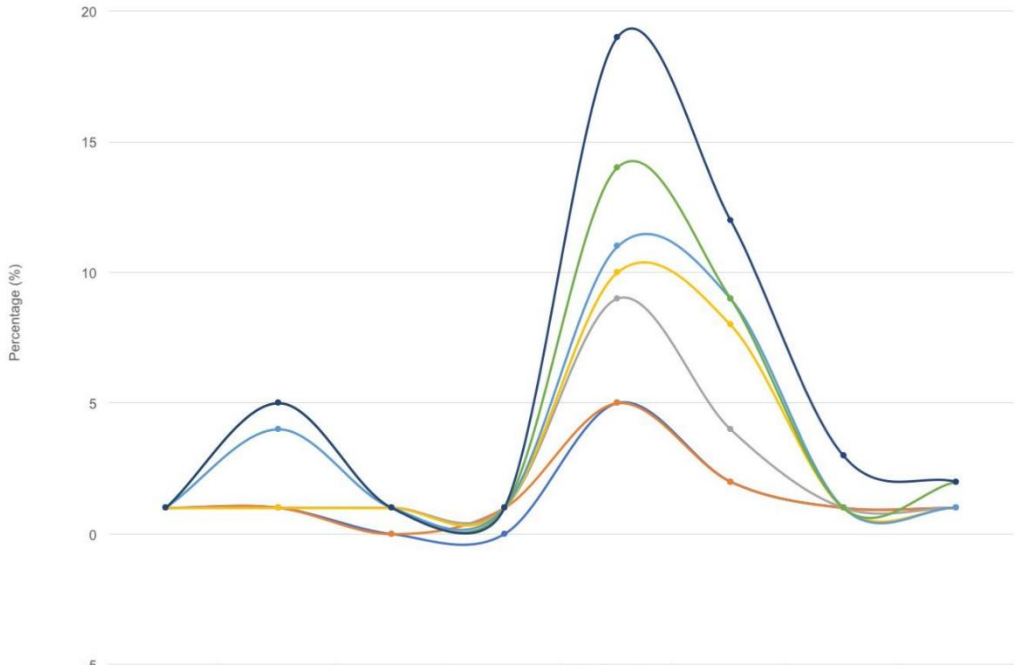

	Isolated AS	Isolated MR	Isolated MS	Mixed aortic valve disease	Mixed mitral and aortic valve disease	Mixed mitral valve disease	MR and AR	No valve lesion
Patchy throughout myocardium	0	0	0	0	5	3	2	0
Patchy midwall	0	1	0	0	3	0	0	1
Patchy linear	0	3	0	0	1	1	0	0
Patchy diffuse	0	0	0	0	1	4	0	0
Linear midwall	0	0	1	0	4	2	0	0
Linear diffuse throughout myocardium	0	0	0	1	0	0	0	0
Diffuse throughout myocardium	1	1	0	0	5	2	1	1

Figure 4.7 Patterns of Late gadolinium enhancement according to valvular lesions

AS, aortic stenosis; MR, mitral regurgitation; MS, mitral stenosis; AR, aortic regurgitation

Table 4.4: Late gadolinium enhancement and additional findings on cardiovascular magnetic resonance

	Subjects (n=44)	***Controls (n=30)***	***P-value***
Presence of LGE n (%)	44 (100)	8 (26.6)	0.001
Valvular enhancement n (%)	29 (65.9)	0(0)	0.001
Myocardial T1 SI ratio, %	0.91 ± 0.51	0.91 ± 0.13	0.98
Myocardial T2 STIR SI ratio, %	1.31 ± 0 .34	1.48 ± 0.22	0.02
Pericardial effusion, n (%)	43 (98)	-	-
Pleural effusion, n (%)	3 (6.8)	-	-
Crypts, n (%)	1 (2.2)	-	-
Incidental findings, n (%)	1 (2.2)	-	-

Continuous data are mean ± SD unless otherwise indicated, late gadolinium enhancement; SI, signal intensity. Values are presented as mean ± standard deviation (SD).

Figure 4.8 below shows the different patterns of enhancement in the PSIR sequence (top row) and corresponding native T1 (middle row) and ECV maps (bottom row). The arrows in B and C indicate circumferential linear and patchy midwall enhancement, respectively.

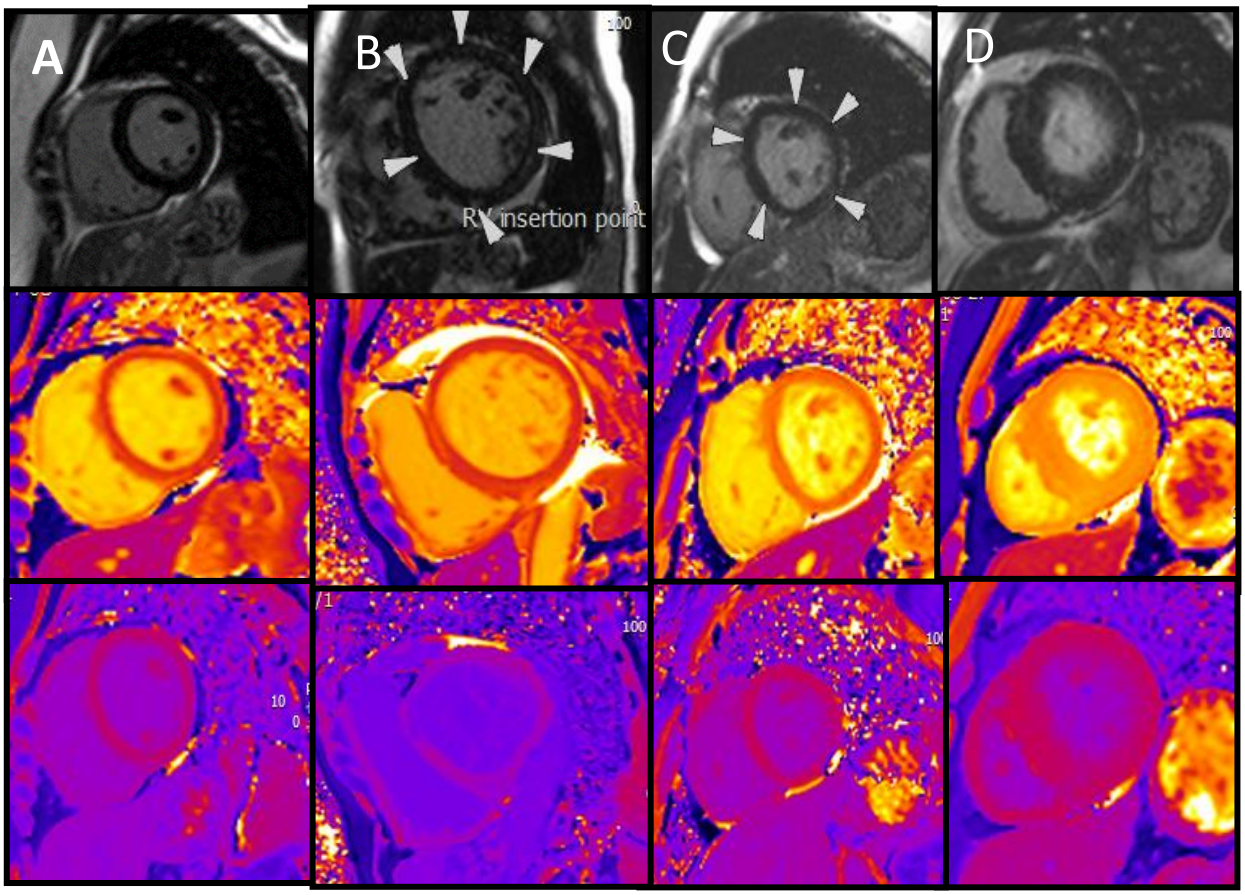

Figure 4.8: Different patterns of late gadolinium enhancement
Top row: PSIR images; Middle row Corresponding T1 Maps; Bottom row –corresponding ECV maps
A: Healthy control with no LGE; B: Linear midwall enhancement in all segments of the LV myocardium indicated by white arrows; C: Patchy midwall enhancement in all segments of the LV myocardium indicated by white arrows
D: Diffuse enhancement involving the entire myocardium
(Permission to use images was granted by all subjects)

Native T1 mapping values were elevated in RHD subjects compared to controls (1279.98 ± 54.14 ms versus 1212.85 ± 33.34 ms, p = 0.004). T2 mapping values were normal, in both subjects and controls, with no significant differences between the two groups. ECV values were elevated in subjects compared to controls, (0.36 ± 0.05% versus 0.28 ± 0.01%, p < 0.000) (Table 4.5).

Table 4.5: Tissue characteristics of the left myocardium

	Subjects (n=44)	Controls (n=30)	P-values
Native T1 mapping, ms	1279.98 ± 54.14	1212.85 ± 33.34	0.004
T2 Mapping, ms	39.26 ± 2.92	38.72 ± 2.19	0.316
ECV, ms	0.36 ± 0.05	0.28 ± 0.01	0.000

Continuous data are mean ± SD, unless otherwise indicated.

ECV, extracellular volume; ms, milliseconds. Values are presented as mean ± SD.

Results showed a significant difference in peak radial, circumferential and longitudinal strain, between subjects and controls ($p < 0.05$). There was no significant difference in peak systolic radial strain rates between subjects and controls ($p = 0.59$), however peak systolic circumferential and longitudinal strain rates showed significant differences between the two groups ($p < 0.05$). Peak diastolic radial, circumferential and longitudinal strain rates were significantly reduced in subjects compared to controls, $p < 0.008$, $p < 0.000$ and $p < 0.000$ respectively (Table 4.6).

Table 4.6: Comparison of myocardial deformational characteristics in subjects and controls

	Subjects (n=44)	***Controls (n=30)***	***P-values***
Peak global radial strain	25.42 ± 9.80	30.80 ± 10.50	0.027
Peak global circumferential strain	-17.70 ± 4.67	-21.06 ± 2.73	0.001
Peak global longitudinal strain	-15.10 ± 6.47	-20.19 ± 2.93	0.000
Peak systolic radial strain rate	1.62 ± 0.94	1.74 ± 0.90	0.592
Peak systolic circumferential strain rate	-0.95 ± 0.25	-1.13 ± 0.23	0.003
Peak systolic longitudinal strain rate	-0.84 ± 0.40	-1.04 ± 0.23	0.018
Peak diastolic radial strain rate	-1.71 ± 0.76	-2.23 ± 0.85	0.008
Peak diastolic circumferential strain rate	0.85 ± 0.31	1.46 ± 0.35	0.000
Peak diastolic longitudinal strain rate	0.72 ± 0.55	1.30 ± 0.34	0.000

Continuous data are mean ± SD unless otherwise indicated

Linear regression analysis was performed to assess the association between peak strain; peak systolic strain rates; peak diastolic strain rates and the following variables: age (Fig. 4.9); native T1 (Fig. 4.9); ECV (Fig. 4.10); and LGE (Fig. 4.11).
There was very weak correlation between age and peak diastolic radial strain rates (R = 0.255, p = 0.02) and a weak negative correlation between age and peak circumferential strain rates (R = -0.334, p = 0.004).

There was a weak positive correlation between native T1 and peak longitudinal strain (R = 0.319, p = 0.006). Weak positive correlations between T1 and peak systolic circumferential and longitudinal strain rates (R = 0.299, p = 0.010 and R = 0.260, p = 0.025) were observed. There was moderate negative correlation between native T1 and peak diastolic circumferential strain rate (R = -0.412, p = 0.001) and weak negative correlation with peak diastolic longitudinal strain rate (R = -0.320, p = 0.005) (Fig. 4.9).

A strong correlation between ECV and peak diastolic circumferential strain rates (R = -0.43, p = 0.00) was found. Similarly, there was a significant correlation between ECV and peak radial strain R = -0.221, p = 0.05, peak circumferential strain R = 0.28 p = 0.017 as well as peak circumferential systolic strain rates, (R = 0.29, p = 0.01) (Fig. 4.10).

There were very weak positive and negative correlations between LGE and all strain parameters (Figure 4.11).

The scatter plots below illustrate the correlation between Native T1 and strain.

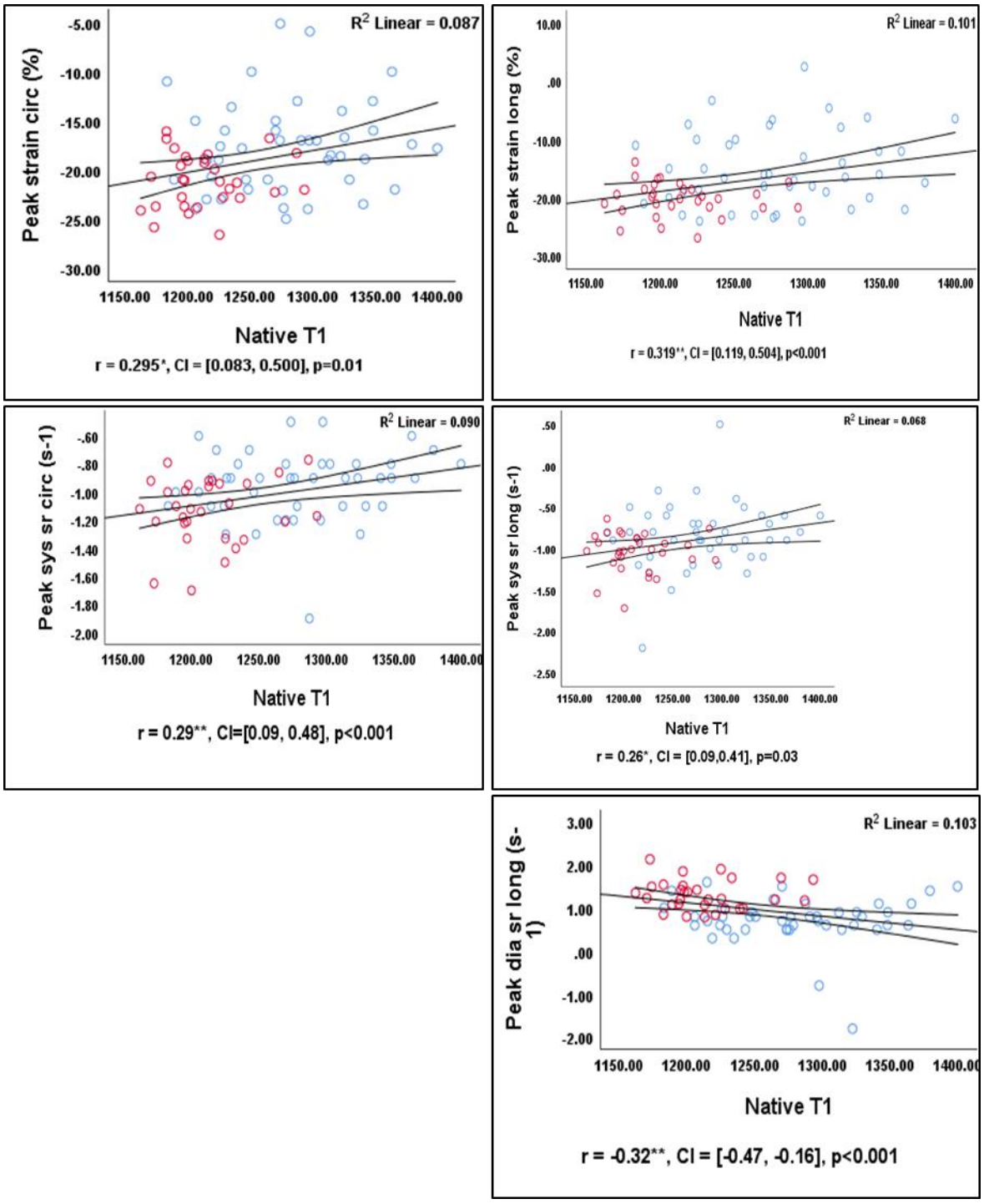

Figure 4.9: Scatter plots illustrating the association between Native T1 and strain parameters

Continuous data are mean ± SD, unless otherwise indicated.

Circ, circumferential; long, longitudinal. Values are presented as mean ± SD.

**** Correlation is significant at the 0.01 level (2-tailed)**

***** Correlation is significant at the 0.05 level (2-tailed)**

The scatter plots below illustrate the correlation between ECV and strain parameters.

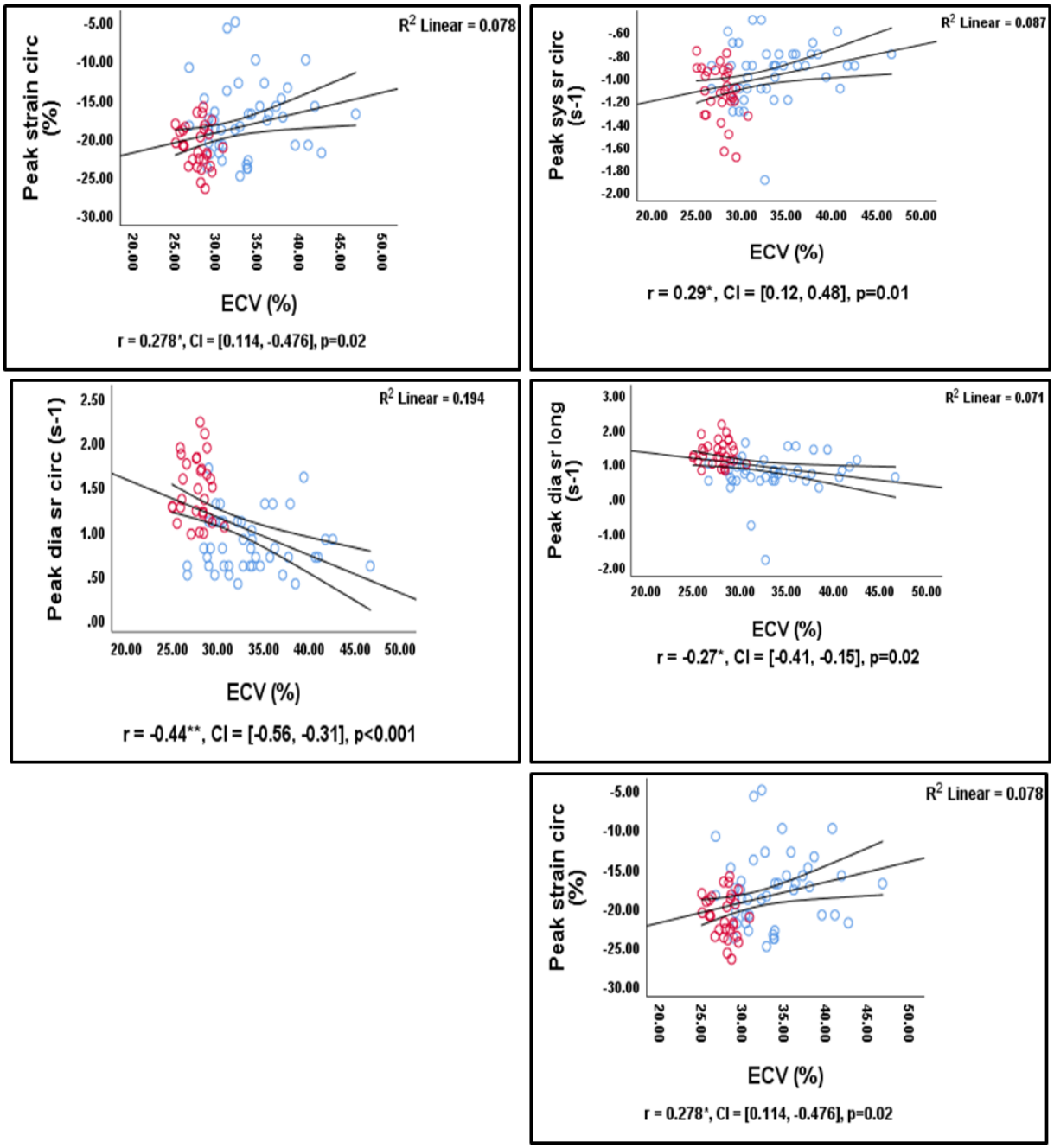

Figure 4.10: Scatter plots illustrating the association between extracellular volume and strain parameters

Continuous data are mean ± SD, unless otherwise indicated.

Circ, circumferential; long, longitudinal. Values are presented as mean ± SD.

**** Correlation is significant at the 0.01 level (2-tailed)**

*** Correlation is significant at the 0.05 level (2-tailed)**

The scatter plots below illustrate the association between LGE and strain parameters.

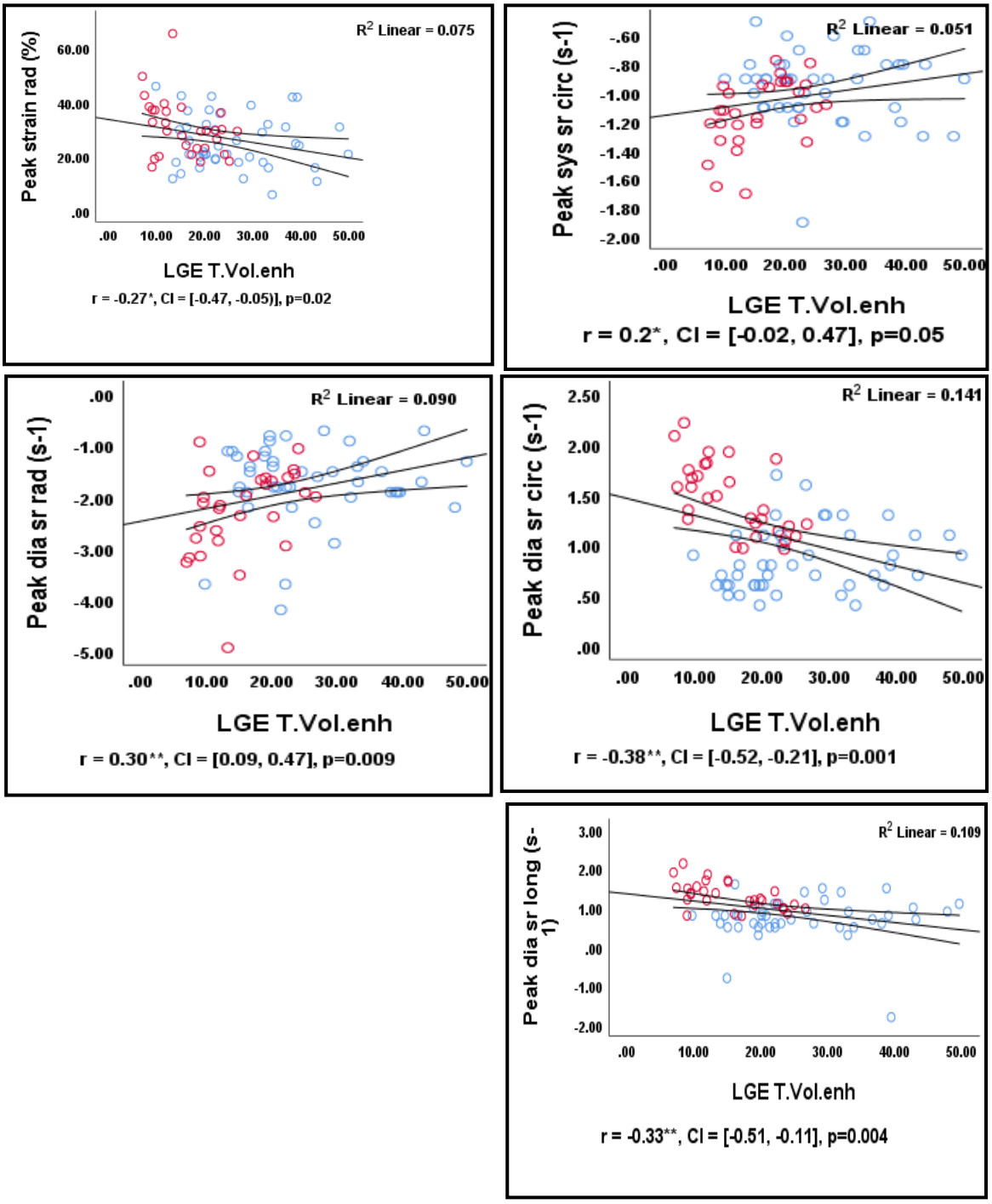

Figure 4.11: Scatter plots illustrating the association between late gadolinium enhancement and strain parameters

Continuous data are mean ± SD, unless otherwise indicated.

Circ, circumferential; long, longitudinal. Values are presented as mean ± SD.

**** Correlation is significant at the 0.01 level (2-tailed)**

*** Correlation is significant at the 0.05 level (2-tailed)**

CHAPTER FIVE
DISCUSSION

CMR is the gold-standard imaging modality for the investigation of cardiovascular disease; it allows extensive delineation of cardiac function, morphology, metabolism, tissue characterisation and haemodynamic outcomes of cardiovascular pathologies (Ntusi, 2018). The primary aim of this study was to document the extent of myocardial fibrosis and structural and functional cardiac changes associated with RHD. A multiparametric CMR protocol was employed to investigate the cardiac changes in subjects with chronic RHD. Forty-four (44) subjects with RHD were investigated and compared with 30 age-, sex-, and ethnicity-matched, healthy controls.

Multiple valve pathologies associated with RHD were observed; with frequent mixed mitral valve disease and mixed mitral and aortic valve disease. Both global LV and RV ejection fractions were reduced in RHD. Myocardial fibrosis, detected by LGE, was present in all study subjects with RHD; majority of subjects had diffuse fibrosis (38%), followed by patchy (36%), and linear fibrosis (26%). Elevated native T1 mapping and ECV values confirmed myocardial fibrosis in RHD subjects.

Globally, RHD is a common and important clinical diagnosis; and is the most common cause of valvular heart disease in children and young adults, particularly in LMIC settings. Although mitral stenosis was the second most common valve lesion observed in this study, it rarely occurred in isolation. Isolated aortic valve disease was similarly infrequent; however, a combination of mitral and aortic valve involvement was seen in half of the cohort. Histopathological studies have previously shown that the mitral valve is most commonly affected, with isolated aortic valve disease occurring in approximately 2% of patients with RHD (Remenyi et. al., 2016). CMR of valve morphology in this study cohort yielded thickened mitral, aortic, tricuspid and pulmonary valves. Tricuspid valve lesions vary by age: in patients younger than 10 years of age, mitral regurgitation is most commonly found; between the ages of 20-30 years, mixed mitral valve disease becomes more prevalent, followed by pure mitral stenosis and aortic valve disease in older individuals (Remenyi et al., 2016). Geographical location could also have played a role in the disease severity, since RHD is a disease aggravated by poverty which is more prevalent in LMICs (Zühlke et al., 2017).

In this cohort, a high incidence of tricuspid regurgitation (TRr) with a small percentage of pulmonary regurgitation was found. All subjects with TRr had either isolated mitral valve disease or mixed mitral and aortic valve disease, likely resulting in functional TRr. The main cause for TRr in MS is elevation of pulmonary pressures and subsequent RV dilation. Functional TRr secondary to left-sided valve disease is usually associated with RV dilatation with or without systolic dysfunction, a sign of advanced disease (Marijon et al., 2012; Remenyi et al., 2016). In this study both left, and right systolic function was decreased in subjects compared to controls, supporting presence of advanced RHD.

Over time, RHD results in adverse cardiac remodelling affecting pathophysiologic parameters such as cardiac output, LV performance, LA size, LV size, LV end-systolic and end-diastolic volumes (Kuruvilla et al., 2013). In this study, there was a statistically significant difference in LV functional parameters (LVEDVi, LVESVi, LVSVi and LVEF) between subjects and controls. While the differences between RHD subjects and controls were statistically significant, the changes to the LV were moderate. The mechanism of LV dysfunction in RHD is secondary to valvular lesions, with haemodynamic adaptations resulting in remodelling, particularly from mitral regurgitation. Repeated myocardial inflammation and myocardial fibrosis also contributes to impairment in LV mechanics and function.

The relationship between valvular lesions and LVEF was assessed and found that subjects with mixed mitral and aortic valve disease (MMAVD) had a LVEF distribution between 38% and 52%. Similarly, subjects with MMVD only, had a LVEF ranging between 39% and 53%. The mean LVEF for both these was 42%. In subjects with mixed aortic valve disease (MAVD), the LVEF was 22%. In this cohort, mixed left sided valvular lesions result in a significant reduction in LVEF. These findings correlate well with what has been described in the literature, ascribing LV remodelling to mitral and aortic valvular dysfunction (Dweck et al., 2012).

Myocardial fibrosis is caused by ECM protein deposits, including collagen and has been shown to be associated with adverse cardiovascular outcomes (Ferreira et al., 2014). LGE is an effective and reproducible method to assess focal myocardial fibrosis and is useful in predicting the prognosis in patients with myocardial infarction and hypertrophic cardiomyopathy. Several studies have shown that the presence of LGE

is a predictor of increased risk of cardiovascular events and increased mortality in patients with cardiomyopathy (Kuruvilla et al., 2013). Myocardial fibrosis was reported much more frequently in this study compared to studies conducted elsewhere. Meel et al., (2018) reported LGE in 18% from a cohort of 22 subjects with chronic rheumatic mitral regurgitation, with varied patterns of LGE including transmural, patchy and sub-epicardial LGE (Meel et al., 2018). In contrast, LGE was present in all the RHD subjects included in this study. There was an almost even split between a diffuse pattern of LGE, observed in (38%) and patchy enhancement (36%). Linear enhancement was observed in 26% of the RHD subject group. Moreover, the distribution of LGE varied in the different segments of the LV myocardium. However, due to the small sample size, researchers were not able to do any statistical correlation between valve lesions and patterns of LGE.

Quantitative analysis of LGE was performed, showing an overall mean volume of 26 ± 10% scarring of total LV myocardial mass in RHD subjects. Apart from the study conducted by Meel et al., there are no other studies quantifying LGE volume fraction in RHD. In a study conducted by Ntusi et al., (2015) in subjects with rheumatoid arthritis, LGE was found in 46% of subjects with quantitative analysis of LGE showing scarring of a small volume of the total LV mass (3.7± 0.4%). Interestingly, this study found LGE in 20% of controls with a predominant linear, midwall pattern of enhancement. None of the healthy controls had a history of heart disease or history of familial cardiac disease, or any co-morbidity that could explain the finding.

Shriki et al., (2011) studied 3 patients with chronic RHD and found LGE in the atrial walls in all 3 patients. In this study, despite a large increase in atria size, LGE was not observed in the atrial walls. Enhancement of the mitral valve was noted in 65.9% subjects in this study. Aortic valve enhancement was seen in 4.5%. The valvular enhancement in these subjects was subtle and differed from the case report described by Samuels et al. (2017) in a woman with acute rheumatic fever (Fig. 2.3) which showed striking enhancement of the mitral, tricuspid and aortic valves with no enhancement in the myocardium. This difference in the degree of enhancement could be due to RHD being a chronic inflammatory process (Ntusi, 2018).

T1 mapping is able to detect diffuse myocardial structural changes, which may be difficult to quantify with LGE (Haaf et al., 2016). This is attributed to the fact that LGE relies on differences in signal intensity between healthy and diseased myocardium, whereas T1 mapping is a pixelwise illustration of absolute T1 relaxation times on a map that circumvents the influence of windowing and nulling (as in LGE), allowing direct T1 quantification. As such, LGE is a reliable method to determine focal fibrosis (Ntusi et al., 2015). However, in the presence of diffuse myocardial fibrosis, LGE becomes problematic as there is no healthy myocardium to use as a reference (Doltra et al., 2013). In this study, mean native T1 values were elevated in RHD patients, which is indicative of myocardial fibrosis. A diagnosis of diffuse fibrosis based on elevated native T1 values is further corroborated by the ECV findings in this study cohort.

In a number of pathological conditions, while the LVEF may be normal, peak systolic strain can be abnormal, indicating sub-clinical LV dysfunction (Mangion et al., 2019). In this study, strain values were impaired in the RHD subject cohort, including abnormal radial, circumferential and longitudinal values for peak global strain, peak systolic strain rates, as well as peak diastolic strain rates. Mangion et al., (2019) reported a poor correlation between age and feature-tracking strain, whereas Taylor et al., (2015), reported an age-related change in circumferential strain in a study conducted on 100 healthy individuals between 20 and 70 years. In this study, a weak correlation between age and all strain parameters was found. Interestingly, a moderate negative correlation between native T1 and peak diastolic circumferential strain rate as well as ECV and peak diastolic circumferential strain rate was found. The interpretation is that the higher the native T1 value, the worse the fibrosis with expansion of the ECM and ECV, which affects LV mechanics and contractility.

5.1 Limitations

This study had several limitations. First, subjects with an eGFR < 30 were excluded due to the small risk of nephrogenic systemic fibrosis, thereby limiting the generalisability of the observations. Second, the sample size of 44 is small, and some interesting regression analyses could not be performed as a consequence. However, despite the small sample size, big differences were noted between RHD and matched controls. Third, the subjects selected all had advanced RHD, likely reflecting the specialised tertiary clinic in which they were seen, with many being assessed for valve replacement surgery. Selection of advanced pathology will have introduced a degree

of selection bias, which would have been avoided by including subjects representing the entire clinical spectrum of RHD. Fourth, the imaging protocol was lengthy and challenging for some subjects with heart failure who had trouble with breath-holding, which had an impact on image quality. Fifth, although no history of claustrophobia was reported, some subjects experienced anxiety when placed into the scanner. One subject withdrew from the study due to anxiety. Finally, there is a paucity of literature on CMR in RHD to draw comparisons from and the existing studies have small sample sizes.

5.2 Conclusions

This study employed a multiparametric CMR approach to investigate the myocardial phenotype of subjects with chronic RHD. Myocardial fibrosis was evident in all subjects, with no distinct pattern of enhancement on LGE imaging. There was an almost even split between subjects with diffuse fibrosis (38%) versus those with patchy fibrosis (36%). Valve lesions noted included MMAVD, MMVD, AR and MR, with frequent observations of thickened valves. Furthermore, there were significant differences in LV functional parameters between subjects and controls. Peak global circumferential, longitudinal and radial strain parameters were abnormal in RHD. Native T1 and ECV were elevated in RHD subjects which correlates well with the finding of increased LGE volume fraction in all. Further research needs to be done to corroborate these findings.

CHAPTER 6
FUTURE DIRECTIONS

The key findings of this study were:

1. Abnormal LV and RV ejection fraction in RHD subjects.
2. Abnormal strain rates in subjects, with moderate to strong correlation between strain and native T1 and ECV respectively, as observed by linear regression analysis.
3. A prevalence of MMVD and mixed mitral and aortic valve disease.
4. A high prevalence of fibrosis throughout the myocardium in all RHD subjects, irrespective of valvular pathology.
5. Increased native T1 and ECV indicating increased myocardial fibrosis.

Based on the above-mentioned key findings and limitations of the present study, the following recommendations are proposed to strengthen CMR findings in RHD:

a. More CMR studies are needed. This will help to establish a statistical correlation between valve lesions and patterns of LGE and to determine whether there is a prevalent pattern of LGE in RHD.
b. CMR registries of RHD are needed.
c. Larger prospective studies, evaluating imaging markers from CMR and their ability to predict clinical events and outcomes, are needed.
d. Comparative studies of CMR parameters and other immunological and molecular biological mechanistic biomarkers are needed.
e. Studies in RHD subjects with contemporaneous agents to assess optimal therapeutic strategies, beyond surgery are needed.
f. Randomised controlled trials in subjects with RHD, testing optimal efficacious therapies, are needed.
g. More advocacy work is needed to ensure that science influences policy and has a measurable impact on individual lives, particularly in LMICs where the disease burden of RHD is highest.

REFERENCES

Abouzeid, M., Wyber, R., La Vincente, S., Sliwa, K., Zühlke, Z., Mayosi, B. & Carapetis, J. 2019. Time to tackle rheumatic heart disease: data needed to drive global policy dialogues. *Global Public Health*, 14(3): 456-468.

Baebler, B. & Emrich, T. 2018. The role of cardiovascular magnetic resonance imaging in rheumatic heart disease. *Clinical and experimental rheumatology*, 36(5):171-176.

Banerjee, T., Mukherjee, S., Ghosh, S., Biswas, M., Dutta, S., Pattari, S., Chatterjee, S. & Bandyopadhyay, A. 2014. Clinical significance of markers of collagen metabolism in Rheumatic Mitral Valve disease. *PloS One,* 9(3): e90527.

Beaton, A. & Carapetis, J. 2015. The 2015 revision of the Jones criteria for the diagnosis of acute rheumatic fever : implications for practice in low-income and middle-income countries. *Heart Asia,* 7(2):7-11.

Beaton, A., Okello, E., Lwabi, P., Mondo, C., McCarter, R. & Sable, C. 2012. Echocardiography Screening for Rheumatic Heart Disease in Ugandan Schoolchildren. *Circulation,* 125(25):3127-3132.

Bulluck, H., Maestrini, V., Rosmini, S., Abdel-Gadir, A., Treibel, T. A., Castelletti, S., Bucciarelli-Ducci, C., Manisty, C. & Moon, J.C. 2015. Myocardial T1 Mapping - Hype or Hope? *Circulation Journal,* 79: 487-494.

Cannaò, P.M., Altabella, L., Petrini, M., Alì, M., Secchi, F. & Sardanelli, F. 2016. Novel cardiac magnetic resonance biomarkers: native T1 and extracellular volume myocardial mapping. *European Heart Journal Supplements,* 18 (Suppl E): 64–71.

Carapetis, J.R, Steer, A.C, Mulholland, E.K. & Weber, M. 2005. The global burden of group A streptococcal diseases. *The Lancet Infectious Diseases,* 5(11):685–694.

Chin, T.K, Hackett, G.L. 2019. *Pediatric Rheumatic Heart Disease*. [Online] Medscape. Available at: https://emedicine.medscape.com/article/891897. [Accessed 23 Jan. 2020].

Doltra, A., Amundsen, B.H., Gebker, R., Fleck, E. & Kelle, S. 2013. Emerging Concepts for Myocardial Late Gadolinium Enhancement MRI. *Current Cardiology Reviews,* 9(3):185–190.

Dougherty, S., Khorsandi, M. & Herbst, P. 2017. Rheumatic heart disease screening: Current concepts and challenges. *Annals of Pediatric Cardiology*, 10(1):39-49.

Duran, C., Sobieszczyk, P.S. & Rybicki, F.J. 2013. Vascular Medicine: A Companion to Braunwald's Heart Disease (Second Edition). *Elsevier*, 166-183.

Dweck, M.R., Joshi, S., Murigu, T., Gulati, A., Alpendurada, F., Jabbour, A., Maceira, A., Roussin, I., Northridge, D.B., Kilner, P.J., Cook, S.A., Boon, N.A., Pepper, J., Mohiaddin, R.H., Newby, D.E., Pennell, D.J. & Prasad, S.K. 2012. Left ventricular remodeling and hypertrophy in patients with aortic stenosis: insights from cardiovascular magnetic resonance. *Journal of cardiovascular magnetic resonance*, *14*(1), 50.

Edwards, N.C., Moody, W.E., Yuan, M., Weale, P., Neal, D., Townend, J.N. & Steeds, R.P. 2014. Valvular Heart Disease Quantification of Left Ventricular Interstitial Fibrosis in Asymptomatic Chronic Primary Degenerative Mitral Regurgitation. *Circulation: Cardiovascular Imaging,* 7(6): 946–953.

Elster, A.D. 2015. *Questions and Answers in MRI. Myocardial T1 Mapping.* [online] *MRIquestions.com*. Available at: http://www.mriquestions.com. [Accessed 2 May 2017].

Ferreira, V. M., Piechnik, S. K., Dall'Armellina, E., Karamitsos, T. D., Francis, J. M., Ntusi, N., Holloway, C., Choudhury, R.P., Kardos, A., Robson, M.D., Friedrich, M.G. & Neubauer, S. 2014. Native T1-mapping detects the location, extent and patterns of acute myocarditis without the need for gadolinium contrast agents. *Journal of Cardiovascular Magnetic Resonance*, 16(1): 36.

Franco, A., Javidi, S. & Ruehm, S.G. 2015. Delayed Myocardial Enhancement in Cardiac Magnetic Resonance Imaging. *Journal of Radiology Case Reports,* 9(6): 6–18.

Friedrich, M.G. 2016. Imaging myocardial inflammation by CMR mapping: good getting better? *European Heart Journal of Cardiovascular Imaging,* 17(2): 134-135.

Friedrich, M.G. & Marcotte, F. 2013. Cardiac Magnetic Resonance Assessment of Myocarditis. *Circulation: Cardiovascular Imaging*, 6:833-839.

Friedrich, M., Sechtem, U., Schulz-Menger, J., Holmvang, G., Alakija, P., Cooper, LT., White, J.A., Abdel-Aty, H., Gutberlet, M., Prasad, S., Aletras, A., Laissy, J.P., Paterson, I., Filipchuk, N.G., Kumar, A., Pauschinger, M. & Liu, P. 2009. International Consensus Group on Cardiovascular Magnetic Resonance in Myocarditis: a JACC White Paper. *Journal of the American College of Cardiology,* 53(17):1475-1487.

Gaasch, W.H, Meyer, T.E. 2008. Left ventricular response to mitral regurgitation: implications for management. *Circulation,* 118(22):2298-2303.

Galvin, J.E., Hemric, M.E., Ward, K. & Cunningham, M.W. 2000. Cytotoxic mAb from rheumatic carditis recognizes heart valves and laminin. *Journal of Clinical Investigation,* 106(2):217-224.

Germain, P., El Ghannudi, S., Jeung, M.Y., Germain, P., Croisille, P., Roy, C. & Gangi, A. 2014. Native T1 Mapping of the Heart – A Pictorial Review. *Clinical Medical Insights: Cardiology,* 8(4): 1–11.

Gewitz, M.H., Baltimore, R.S., Tani, L.Y., Sable, C.A., Shulman, S.T., Carapetis, J., Remenyi, B., Taubert, K., Bolger, A.F., Beerman, L., Mayosi, B.M., Beaton, A., Pandian, N.G. & Kaplan, E.L. 2015. Revision of the Jones criteria for the diagnosis of acute rheumatic fever in the era of Doppler echocardiography. A scientific statement from the American heart association. *Circulation,* 131(20): 1806–1818.

Greenwood, J. P., Broadbent, D. & Biglands, J. 2015. *Cardiovascular Magnetic Resonance.* In: Physics for Clinicians Pocket Guide. [online] Available at: http://www.cmr-guide.com [Accessed 5 May 2018]

Guilherme, L., Ramasawmy, R. & Kalil, J. 2007. Rheumatic Fever and Rheumatic Heart Disease : genetics and pathogenesis. *Scandinavian Journal of Immunology*, 66: 199-207.

Haaf, P., Garg, P., Messroghli, D.R., Broadbent, D.A., Greenwood, J.P. & Plein, S. 2016. Cardiac T1 Mapping and Extracellular Volume (ECV) in clinical practice : a comprehensive review. *Journal of Cardiovascular Magnetic Resonance,* 18(89): 1-12.

HPCSA (Health Professions Council of South Africa). 2008. *HPCSA Ethical guidelines for good practise in the health care professions.* [online] Available at: <https://www.hpcsa.co.za/Uploads/Professional_Practice/Ethics_Booklet.pdf> [Accessed 18 May 2018].

Irlam, J., Mayosi, B.M., Engel, M., Gaziano, T.A. 2013. Primary Prevention of Acute Rheumatic Fever and Rheumatic Heart Disease with Penicillin in South African Children with Pharyngitis: a cost-effectiveness analysis. *Circulation: Cardiovascular Quality and Outcomes*, 6: 343-351.

Karthikeyan, G., Zühlke, L., Engel, M.,Rangarajan, S., Yusuf, S.,Teo, K & Mayosi, B.M. 2017. Rationale and design of a Global Rheumatic Heart Disease Registry: the REMEDY study. *American Heart Journal,* 163(4): 534-540.

Kuruvilla, S., Adenaw, N., Katwal, A.B., Lipinski, M.J., Kramer, C.M. & Salerno, M. 2013. Late Gadolinium Enhancement on Cardiac Magnetic Resonance Predicts Adverse Cardiovascular Outcomes in Non-ischemic Cardiomyopathy: a systemic review and meta-analysis. *Circulation: Cardiovascular Imaging*, 7(2): 250-258.

Luiza, G. & Jorge, K. 2013. Rheumatic heart disease: molecules involved in valve tissue inflammation leading to the autoimmune process and anti-S. Pyogenes vaccine. *Frontiers in Immunology*, 4: 352.

Mangion, K., Burke, N.M.M., Mccomb, C., Carrick, D., Woodward, R. & Berry, C. 2019. Feature-tracking myocardial strain in healthy adults- a magnetic resonance study at 3 .0 tesla. *Scientific Reports*, 9(3239): 1-9.

Marciniak, A., Claus, P., Sutherland, G.R., Marciniak, M., Karu, T., Baltabaeva, A., Merli, E., Bijnens, B. & Jahangiri, M. 2007. Changes in systolic left ventricular function in isolated mitral regurgitation. A strain rate imaging study. *European Heart Journal,* 28: 2627-2636.

Marijon, E., Mirabel, M., Celermajer, D.S. & Jouven, X. 2012. Rheumatic Heart Disease. *The Lancet,* 379(9819): 953-964.

Martin, W.J., Steer, A.C., Smeesters, P.R., Keeble, J., Inouye, M., Carapetis, J., & Wicks, I.P. 2015. Post-infectious group A streptococcal autoimmune syndromes and the heart. *Autoimmunity Reviews*, 14(8): 710-725.

Martins, C.O., Demarchi, L., Ferreira, F.M., Pomerantzeff, P.M., Brandao, C., Sampaio, R.O., Spina, G.S., Kalil, J., Cunha-Neto, E., & Guilherme, L. 2017. Rheumatic Heart Disease and Myxomatous Degeneration: differences and similarities of valve damage resulting from autoimmune reactions and matrix disorganization. *PloS one*, 12(1): e0170191.

Mayosi, B.M. 2014. The challenge of silent Rheumatic Heart Disease. *The Lancet Global Health,* 2(12): 677-678.

McDonald, M., Brown, A., Noonan, S., & Carapetis, J.R. 2005. Preventing recurrent rheumatic fever: the role of register-based programmes. *Heart: British Cardiac Society,* 91(9): 1131-1133.

Meel, R., Nethononda, R., Libhaber, E., Dix-peek, T., Peters, F. & Essop, M. 2018. Assessment of myocardial fibrosis by late gadolinium enhancement imaging and biomarkers of collagen metabolism in chronic rheumatic mitral regurgitation. *Cardiovascular Journal of Africa,* 29(3): 150-154.

Moodley, J., Pattinson, R.C., Bennun, M. & Cronje, H.S. 2000. A review of maternal deaths in South Africa during 1998. *South African Medical Journal,* 90(4): 367-373.

Moxon, T.A., Reed, P., Jelleyman, T., Reed, P., Jackson, C. & Lennon, D. 2017. Is a rheumatic fever register the best surveillance tool to evaluate rheumatic fever control in the Auckland region? *New Zealand Medical Journal,* 130(1460): 48-62.

Mutnuru, P.C., Singh, S.N. & Perubhotla, L.M. 2016. Cardiac MR Imaging in the Evaluation of Rheumatic Valvular Heart Diseases. J*ournal of Clinical and Diagnostic Research,* 10(3): TC06-TC09.

Myerson, S.G., Francis, J. & Neubauer, S. 2010. *Oxford Specialist Handbook in Cardiology: Cardiovascular Magnetic Resonance.* Oxford: Oxford University Press, 18-19.

Nacif, M.S., Zavodni, A., Kawel, N., Choi, E-Y., Lima, J.A.C. & Bluemke, D.A. 2012. Cardiac magnetic resonance imaging and its electrocardiographs (ECG): tips and tricks. *The International Journal of Cardiovascular Imaging,* 28:1465-1475.

Neubauer, S. 2018. Cardiovascular magnetic resonance imaging Key points. *Medicine*, 46(8): 480-487.

Norton, P.T., Nacey, N.C., Caovan, D.B., Gay, S.B., Kramer, C.M., Bryan S. & Jeun, B.S. 2013. *Cardiac MRI: The Basics.* [online] Available at: https**://**www**.**med-ed**.**virginia**.**edu**/**courses**/**rad**/**cardiacmr**/**index**.**html. [Accessed 1 Apr. 2018].

Ntusi, N.A.B. 2018. Cardiovascular magnetic resonance imaging in rheumatic heart disease - Editorial. *Cardiovascular Journal of Africa*, 29(3): 135-138.

Ntusi, N.A.B., Piechnik, S.K., Francis, J.M., Ferreira, V.M., Matthews, P.M., Robson, M.D., Wordsworth, P.B., Neubauer, S. & Karamitsos, T. D. 2015. Diffuse myocardial fibrosis and inflammation in rheumatoid arthritis: insights from CMR T1 mapping. *Journal of the American College of Cardiology: Cardiovascular Imaging*, 8(5): 526-536.

Prasad, A., Kumar, S., Singh, B.K. & Kumari, N. 2017. Mortality Due to Rheumatic Heart Disease in Developing World: a preventable problem. *Journal of Clinical and Experimental Cardiology*, 8(3): 2155-9880.

Remenyi, B., ElGuindy, A., Smith, S.C., Yacoub, M., Holmes, D.R. 2016. Valvular aspects of rheumatic heart disease. *The Lancet,* 387(10025): 1335–1346.

Remenyi, B., Carapetis, J., Wyber, R., Taubert, K. & Mayosi, B.M. 2013. Position statement of the World Heart Federation on the prevention and control of rheumatic heart disease. *Nature Reviews Cardiology*, 10(5): 284-292.

Rheumatic Heart Disease Australia. 2012. *The Australian guideline for prevention , diagnosis and management of acute rheumatic fever and rheumatic heart disease.* (2nd edition). Quick reference guides. [online] Available at: https://www.rhdaustralia.org.au/arf-rhd-guideline. [Accessed 23 Mar. 2019].

Roller, F.C., Harth, S., Schneider, C. & Krombach, G.A. 2015. T1, T2 Mapping and Extracellular Volume Fraction (ECV): Application, Value and Further Perspectives in Myocardial Inflammation and Cardiomyopathies. *Fortschritte Röntgenstrahlen*, 187: 760–770.

Rubin, E. 2001. *Essential Pathology*. 3rd ed. Philadelphia: Lippincot Williams & Wilkins, 467-468.

Samuels, P., Chin, A., Ntsekhe, M. & Ntusi N.A.B. 2017. *CMR unravels the pathophysiology of heart block in a young woman.* Cardiovascular Magnet Resonance Congress South Africa 2017 (abstract). [online] Available at: http://www.cubic.uct.ac.za/sites/default/files/image_tool/images/217/SCMR%20Abstract%20Petty. pdf. [Accessed 04 Apr. 2019].

Seckeler, M.D., & Hoke, T.R. 2011. The worldwide epidemiology of acute rheumatic fever and rheumatic heart disease. *Clinical Epidemiology,* 3: 67-84.

Sepulveda, D.L., Calado, E.B., Albuquerque, E., Rodrigues, A., Siqueira, M.E.M., Lapa, C., Saraiva, L., Mochiduky, R., Sobral, D. & Uellendahl, M. 2013. Cardiac magnetic resonance in acute rheumatic fever. *Springer Link,* 15(Suppl 1): 14-15.

Shriki, J., Talkin, B., Thomas, I.C., Farvid, A. & Colletti, P.M. 2011. Delayed gadolinium enhancement in the atrial wall: a novel finding in 3 patients with rheumatic heart disease. *Texas Heart Institute Journal,* 38(1): 56-60.

Smith, R.C. & Lange, R.C. 1997. *Understanding magnetic resonance imaging.* New York: CRC Press.

Suinesiaputra, A., Bluemke, D.A., Cowan, B.R., Friedrich, M.G., Kramer, C.M., Kwong, R., Sven Plein, S., Schulz-Menger, J., Westenberg, J.J.M., Young, A.A. & Nagel, E. 2015. Quantification of LV function and mass by cardiovascular magnetic resonance: multi-center variability and consensus contours. *Journal of Cardiovascular Magnetic Resonance,* 17: 63.

Suthahar, N., Meijers, W.C., Silljé, H.H. W. & De Boer, R.A. 2017. From Inflammation to Fibrosis - Molecular and Cellular Mechanisms of Myocardial Tissue Remodelling and Perspectives on Differential Treatment Opportunities. *Current Heart Failure Reports*, 14: 235-250.

Taylor, R.J., Moody, W.E., Umar, F., Edwards, N.C., Taylor, T.J., Stegemann, B., Townend, J.N., Hor, K.N., Steeds, R.P., Mazur, W. & Leyva, F. 2015. Myocardial strain measurement with feature-tracking cardiovascular magnetic resonance: normal values. *European Heart Journal - Cardiovascular Imaging,* 16(8): 871-881.

Unger, P., Clavel, M., Lindman, B.R., Mathieu, P. & Pibarot, P. 2017. Pathophysiology and management of multivalvular disease. *Nature Reviews Cardiology,* 13(7): 429-440.

Westbrook, C., Kaut-Roth, C. & Talbot, J. 2005. *MRI in Practice*. 3rd ed. Oxford: Blackwell Publishing.

WHO (World Health Organization). Int. 2001. Rheumatic fever and Rheumatic Heart Disease. [online] Available at: https://www.who.int/cardiovascular_diseases/publications/trs923/en [Accessed 1 May 2019].

WMA (World Medical Association). 2013. *Declaration of Helsinki – Ethical Principles for Medical Research Involving Human Subjects*. [online] Available at: <https://www.wma.net/policies-post/wma-declaration-of-helsinki-ethical-principles-for-medical-research-involving-human-subjects/> [Accessed 5 Apr. 2017].

Zühlke, L.J., Beaton, A., Engel, M.E., Hugo-Hamman, C.T., Karthikeyan, G., Katzellenbogen, J.M., Ntusi, N.A.B., Ralph, A.P., Saxena, A., Smeesters, P.R., Watkins, D., Zilla, P. & Carapetis, J. 2017. Group A Streptococcus, Acute Rheumatic Fever and Rheumatic Heart Disease Epidemiology and Clinical Considerations. *Current Treatment Options Cardiovascular Medicines*, 19(2): 15-48.

Zühlke, L.J, Engel, M.E., Karthikeyan, G., Rangarajan, S., Mackie, P., Cupido, B., Mauff, K., Islam, S., Joachim, A., Daniels, R., Francis, V., Ogendo, S., Gitura, B., Mondo, C., Okello, E., Lwabi, P., Al-Kebsi, M.M., Hugo-Hamman, C., Sheta, S.S., Haileamlak, A., Daniel, W., Dejuma Y. Goshu, D.Y., Abdissa, S.G., Desta, A.G., Shasho, B.A., Begna, D.M., ElSayed, A., Ibrahim, A.S., Musuku, J., Bode-Thomas, F., Okeahialam, B.N., Ige, O., Sutton, C., Misra, R., Fadl, A.A., Kennedy, N., Damasceno, A., Sani, M., Ogah, O.S., Olunuga, T., Elhassan, H.H.M., Mocumbi, A.O., Adeoye, A.M., Mntla, P., Ojji, D., Mucumbitsi, J.,Teo, K.,Yusuf, S. & Mayosi, B.M. 2015. Characteristics, complications, and gaps in evidence-based interventions in rheumatic heart disease: the global rheumatic heart disease registry (the REMEDY study). *European Heart Journal,* 36(18): 1115–1122.

Zühlke, L.J., Engel, M.E., Watkins, D. & Mayosi, B.M. 2015. Incidence, prevalence and outcome of rheumatic heart disease in South Africa: a systematic review of contemporary studies. *International Journal of Cardiology,* 199: 375-383.

Zühlke, L.J., Watkins, D. & Engel, M. 2014. Incidence, prevalence and outcomes of rheumatic heart disease in South Africa: a systematic review protocol. *British Medical Journal Open,* 4(6): 004844.

Zühlke, L. J. & Engel, M. E. 2013. The Importance of Awareness and Education in Prevention and Control of RHD. *Global Heart,* 8(3): 235-239.

Zühlke, L.J. & Karthikeyan, G. 2013. Primary Prevention for Rheumatic Fever. *Global Heart,* 8(3): 221–226.

APPENDIX A: ETHICS CERTIFICATE CAPE PENINSULA UNIVERSITY OF TECHNOLOGY

Cape Peninsula
University of Technology

HEALTH AND WELLNESS SCIENCES RESEARCH ETHICS COMMITTEE (HW-REC)
Registration Number NHREC: REC- 230408-014

P.O. Box 1906 • Bellville 7535 South Africa
Symphony Road Bellville 7535
Tel: +27 21 959 6917
Email: sethn@cput.ac.za

2 August 2017
REC Approval Reference No:
CPUT/HW-REC 2017/H23

Dear Petronella Samuels

Re: APPLICATION TO THE HW-REC FOR ETHICS CLEARANCE

Approval was granted by the Health and Wellness Sciences-REC on 15 June 2017 to Ms Samuels for ethical clearance. This approval is for research activities related to student research in the Department of Medical Imaging and Therapeutic Science at this Institution.

TITLE: Multi-parametric cardiovascular magnetic resonance characterization of myocardial inflammation in patients with rheumatic heart disease

Supervisor: Mr A Speelman and Prof N Ntusi

Comment:

Approval will not extend beyond 3 August 2018. An extension should be applied for 6 weeks before this expiry date should data collection and use/analysis of data, information and/or samples for this study continue beyond this date.

The investigator(s) should understand the ethical conditions under which they are authorized to carry out this study and they should be compliant to these conditions. It is required that the investigator(s) complete an **annual progress report** that should be submitted to the HWS-REC in December of that particular year, for the HWS-REC to be kept informed of the progress and of any problems you may have encountered.

Kind Regards

Mr. Navindhra Naidoo
Chairperson – Research Ethics Committee
Faculty of Health and Wellness Sciences

APPENDIX B: ETHICS CERTIFICATE UNIVERSITY OF CAPE TOWN

UNIVERSITY OF CAPE TOWN
Faculty of Health Sciences
Human Research Ethics Committee

Room E52-24 Old Main Building
Groote Schuur Hospital
Observatory 7925
Telephone [021] 404 7682 • **Facsimile** [021] 406 6411
Email: nosi.tsame@uct.ac.za
Website: www.health.uct.ac.za/fhs/research/humanethics/forms

21 April 2017

HREC REF: 234/2017

Prof N Ntusi
Medicine
Old Main Building

Dear Prof Ntusi

PROJECT TITLE: MULTIPARAMETRIC CARDIOVASCULAR MAGNETIC RESONANCE CHARACTERISATION OF MYOCARDIAL INFLAMMATION IN PATIENTS WITH RHEUMATIC HEART DISEASE-MSc-candidate-P Samuels

Thank you for submitting your study to the Faculty of Health Sciences Human Research Ethics Committee for review.

It is a pleasure to inform you that the HREC **has formally approved** the above-mentioned study.

Approval is granted for one year until the 30th April 2018.

Please submit a progress form, using the standardised Annual Report Form if the study continues beyond the approval period. Please submit a Standard Closure form if the study is completed within the approval period.
(Forms can be found on our website: www.health.uct.ac.za/fhs/research/humanethics/forms)

We acknowledge that Ms P Samuels will be involved in this study.

Please note that for all studies approved by the HREC, the principal investigator **must** obtain appropriate institutional approval before the research may occur.

Please quote the HREC REF in all your correspondence.

Please note that the ongoing ethical conduct of the study remains the responsibility of the principal investigator.

Yours sincerely

PROFESSOR M BLOCKMAN
CHAIRPERSON, FHS HUMAN RESEARCH ETHICS COMMITTEE
Federal Wide Assurance Number: FWA00001637,
Institutional Review Board (IRB) number: IRB00001938

HREC 234/2017

APPENDIX C: APPROVAL LETTER FROM CAPE UNIVERSITIES BODY IMAGING CENTRE

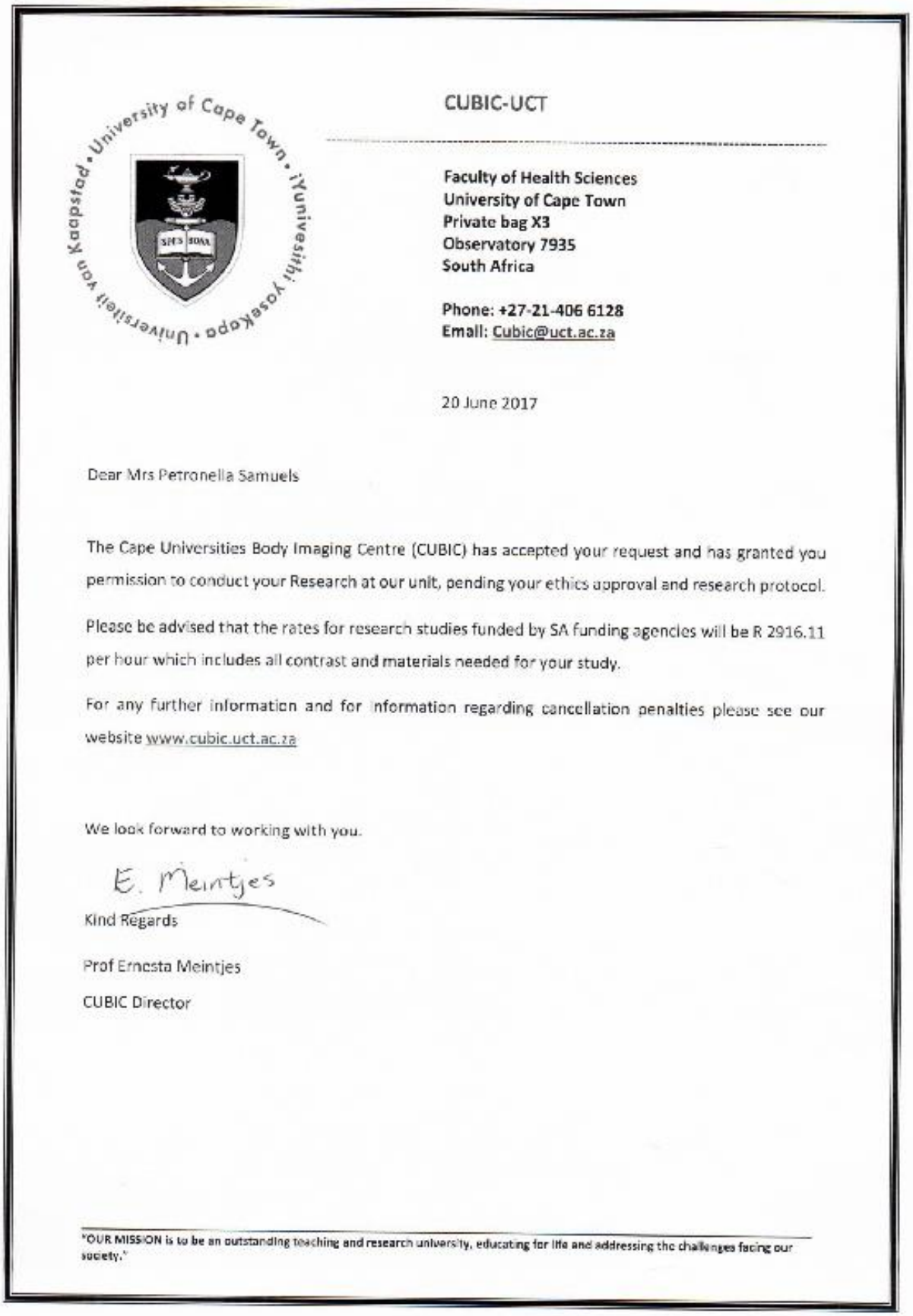

CUBIC-UCT

Faculty of Health Sciences
University of Cape Town
Private bag X3
Observatory 7935
South Africa

Phone: +27-21-406 6128
Email: Cubic@uct.ac.za

20 June 2017

Dear Mrs Petronella Samuels

The Cape Universities Body Imaging Centre (CUBIC) has accepted your request and has granted you permission to conduct your Research at our unit, pending your ethics approval and research protocol.

Please be advised that the rates for research studies funded by SA funding agencies will be R 2916.11 per hour which includes all contrast and materials needed for your study.

For any further information and for information regarding cancellation penalties please see our website www.cubic.uct.ac.za

We look forward to working with you.

E. Meintjes

Kind Regards

Prof Ernesta Meintjes

CUBIC Director

APPENDIX D: PATIENT INFORMATION LEAFLET

PARTICIPANT INFORMATION SHEET
MULTIPARAMETRIC CARDIOVASCULAR MAGNETIC RESONANCE CHARACTERISATION OF MYOCARDIAL INFLAMMATION IN PATIENTS WITH RHEUMATIC HEART DISEASE

You are invited to take part in a research study. Before you decide, it is important for you to understand why the research is being done and what it will involve. Please take time to read the following information carefully and discuss it with friends, relatives and your doctor, if you wish. This leaflet will tell you the purpose of the study, what will happen to you when you take part and gives you detailed information about the conduct of the study.
Ask us if there is anything that is not clear or if you would like more information. Thank you for reading this.

What is the purpose of the study?

Patients with rheumatic heart disease (RHD) have inflammation of the heart valves that will cause the valves to become narrow and thickened or leaky. It may cause disease of the heart muscle which may cause the heart to get bigger and also weaken the muscle of the heart muscle. The inflammation of the heart valves may also be seen as inflammation in the muscle of the heart, where the disease causes irregular flare up of inflammation. We would like to do the MRI scan to determine how often the heart valves get inflamed and also check for any damage in the heart muscle in patients with rheumatic heart disease. In the future, we will also be interested to assess the connection between the inflammation of the heart muscle and scarring on MRI with cardiovascular results.
If you take part in this study, you will be seen at a visit, where you will be examined, and undergo a resting electrocardiogram (ECG). If you have not had a recent ultrasound scan of the heart, you will be offered one. We will then examine the structure and function of your heart with an MRI scan. You will not be asked to take any additional long-term pills or alter your regular medication in any way.

Why have I been invited?

You have been invited because you have previously been diagnosed with rheumatic heart disease.

Do I have to take part?

It is up to you to decide whether or not to take part. If you decide to take part, you are free to withdraw consent at any time without giving a reason. Your decision will not affect further treatment for your condition. If you decide that you no longer wish to continue with the study, we would still keep all the test results that we got from you up to the point of your withdrawal.

What would happen to me if I take part?

You would attend a visit that will last about 2 hours. At this visit, we will ask some general questions about your health and regular medication. After that, we will do a quick check of your pulse, blood pressure, weight and height. We will also do an ECG trace of your heart's electrical impulse. After that, we may perform an ultrasound scan of your heart. We will then scan your heart, using cardiac MRI. If your ultrasound or MRI scan suggests abnormalities, we will advise your doctors to refer you to a cardiologist for review.

Below, all the above-mentioned tests are discussed in a little bit more detail:

1. **Clinical assessment**

The assessment will start by asking you a set of questions about your health and previous medical conditions, using a structured questionnaire. The physical examination will include measurement of your pulse, blood pressure, weight and height, as well as an examination of the heart and the vessels.

2. **The heart MRI scan**

The MRI scan of your heart will be the most important part of this study and will last about 60 minutes. MRI scans are painless but involve the use of a strong magnetic field, so if you have any of the following, you would not be suitable for a scan, and would not be able to take part in this study:

- a permanent pacemaker

- metal clips in blood vessels of the brain
- an injury to the eye involving fragments of metal
- shrapnel injuries, bullet fragments
- other metal or electronic implants affected by the magnetic field
- neurostimulators
- cochlear implant
- insulin pump

The MRI scanner is shaped like a doughnut, the hole inside is about 70 centimetres wide, with a table that slides in and out.

You will be asked to change into a hospital gown and lie on your back for the scan. We will clean your skin with gel to put special ECG stickers on your chest. Your heart rate will be measured during the scan and it is important to lie very still while your heart is being scanned. You will also be asked to breathe in and out and hold your breath for several seconds for most of the scans. Pictures of the heart are created using a magnetic field, radio waves and computers. When images are being taken, the MRI scanner makes a loud noise, and you will be provided with earphones to protect your ears. It is important that you lie still for the duration of the scan. We will give you a buzzer that you can squeeze should you feel any pain or discomfort during the scan.
To do a complete assessment of the heart, we need to examine the blood circulation and your heart muscle to check for inflammation and scarring. We also need to assess the appearance of the tissue of the heart. In order to do this, we shall inject some contrast dye, called gadolinium, through a drip into your arm. This will only be done towards the last 15 minutes of the scan.

The Electrocardiogram (ECG)

We will take an electrocardiogram (ECG) of your heart which will last about 5 minutes. An ECG is a tool that uses surface electrodes on certain points on your chest and arms to monitor the electrical properties of your heart.

3. The ultrasound of the heart (15-20 minutes)

An echocardiogram or ultrasound of your heart is a safe and painless procedure to study heart structure and function. You will be asked to lie on a couch on your left side, and a probe will be placed on your chest. Lubricating jelly is used so the probe makes good contact with the skin. Ultrasound waves then create images of your heart on the scanner monitor. It normally takes 15-20 minutes to acquire these images.

What about travel expenses?

We will reimburse travel expenses to and from the hospital. Lunch will be provided or reimbursed.

What will I have to do, if I agree to take part in this study?

- Attend a visit at Groote Schuur Hospital for the assessment, blood tests and for the scans.

- Consent to taking part in this study by signing a form.
- We will ask that you do not have anything to eat 4-6 hours before the visit.
- Undergo the procedures as described above.

Are there any other possible risks from taking part?
The scanning is done using an MRI scanner which is also used routinely in clinical practice to acquire images of various body parts. MRI scans are safe, non-invasive and do not involve any ionising radiation (X-rays). Some people find the space limitation in the scanner uncomfortable, but you will be given a chance to see the scanner to make sure that you are comfortable in it before the study starts. The scan is noisy, and we provide headphones to protect your ears. The whole time that you are in the scanner you will be given a buzzer which you will be able to use at any time if you wish to stop the study. As the scanner consists of a powerful magnet, it may attract certain metallic objects. You must not have a scan if you have had metallic objects or medical devices (e.g. pacemaker) or surgical implants such as stainless-steel screws, hip replacements inserted into your body during an operation. Please inform us if you have any of these metal implants anywhere in your body. MRI is safe in pregnancy, because this is a research study, as a precaution we advise you to tell us if there is any chance you might be pregnant. The doctor or radiographer will go through a list of possible risks with you before you go into the scanner.
In the unlikely event of us seeing any structural abnormalities on your MRI scan, a member of our research team will discuss the implications with you, and, with your permission, your doctor may be notified. However, it is important to note that we do not carry out scans for diagnostic purposes, and therefore these scans are not a substitute for a clinical appointment. Rather, our scans are intended for research purposes only. Some people find having a drip in their arm uncomfortable and there can be bruising at the site of needle entry. Our staff is trained in drip insertion and we will make sure you are as comfortable as possible.
Gadolinium, the dye used for the MRI scans, has been in clinical use for over 20 years. As the dye is being injected, some people report a sensation of warmth at the injection site. It is unusual to feel pain, and in this case, we would stop the injection immediately. Rarely, some people feel slightly nauseous or have a metallic taste following the injection, but vomiting is very rare. Occasionally, people have developed a rash; however, severe allergic reactions are very rarely experienced. Again, this dye is injected through a drip in the arm. There is no pain associated with the injection at the site. There is a small risk of an allergic reaction to the dye.
ECG and ultrasound are safe, non-invasive tests, with no known serious risks/harm. Rarely, individuals having either test may develop an allergic reaction to placement of electrodes that results in a mild rash. This rash disappears in a few days without any treatment.
It is important to note that in a large-volume MRI centre like Groote Schuur Hospital, where our experienced staff has been doing MRI scans for many years, the risk of harm from the MRI and other tests is exceedingly small.
What are the possible benefits?
There is no direct benefit for you as an individual taking part in this study. We hope that by studying people with your condition using cardiac MRI, we may be able to improve understanding of this condition and help to inform screening and or treatment of future patients.

What happens when the research study stops?

The end of the study will not affect the care you receive from your doctors. The end of the study will mark the official end of your participation in this project. Copies of any publications connected to this study will be available on request from Professor Ntusi. Please inform us should you wish to have copies of the findings of this research project.
Will my taking part in the study be kept confidential?
Yes. We will follow ethical and legal practice and all information about you will be handled in confidence. If you take part in the study, some of the data collected from the study would be looked at by authorized persons from the University of Cape Town, to check that the study is being carried out correctly. All investigators have a duty of confidentiality to you as a research participant, and nothing that could reveal your identity would be disclosed outside the research site. The data collected from the study will be recorded anonymously and you would not be identifiable from this.

What if relevant new information becomes available?
Sometimes, we (the study investigators) get new information about the procedures being studied. If this happens, one of us will tell you and discuss whether you should continue in the study. If there is sufficient evidence to suggest you may be harmed from participating in this study, the study could be stopped.

Unexpected findings on your scan
In the unlikely event of us seeing any structural abnormalities on your MRI scan, a designated clinical specialist will discuss the implications with you and may arrange for further investigations as necessary. However, it is important to note that we do not carry out scans for diagnostic purposes, and therefore these scans are not a substitute for a clinical appointment. Rather, our scans are intended for research purposes only. So, if we find anything unusual, it would be appropriate for us to contact your GP/specialist so that they can arrange on-going clinical care for you. But we would only do this after we and the specialist had discussed your options and gained your permission.

What will happen if I don't want to carry on with the study?

You are free to withdraw from the study at any time. Anonymised data will be kept till the point you choose to end your participation in the study. Data collected till the point of your withdrawal will be included in the analysis.

What will happen to the results of the research study?
We anticipate that the results will be published in a scientific journal for the benefit of the wider medical community. However, individual patients will not be identified in any publication and your personal and clinical details will remain strictly confidential. Any scientific publications arising from the study will be available on request to all participants. You would have no legal right to a share of any profits that may arise from the research.

Will your test results be shared with you?
We will show you the images we acquire from the ultrasound and MRI scans when we finish performing the scans. The results of the other tests will only be available on publication of the results. If however, results of any of the tests are grossly abnormal, we will contact you to discuss these with you before suggesting a course of action and contacting your doctor/specialist.

Who is organising and funding the research?
The study is organised and conducted by researchers from the University of Cape Town and Groote Schuur Hospital. The studies are funded, in part, by a grant from the National Research Foundation of South Africa.

Who has reviewed the study?

The University of Cape Town Human Research Ethics Committee as well as the Research Ethics Committee of the Cape Peninsula University of Technology has reviewed and approved the study.

Further information and contact details

Should you wish to know more about any aspects of this study, please contact:
Professor Ntusi at: (021) 406 6200; or
Mrs Petronella Samuels at: (021) 406 6132

APPENDIX E: MRI COMPATIBILITY CHECKLIST

Cape Universities Body Imaging Centre (CUBIC)
University of Cape Town

MRI Participant Screening Form

Study: _____
Participant Code: _____
Date Of Birth: _____ Weight: _____
Height: _____

The following information is very important to ensure your safety and to prevent any interference during the MR procedure.

Please answer the following questions (mark with a X):

		Yes	No	Don't Know
1.	Do you have a cardiac pacemaker/defibrillator?			
2.	Do you have a neuro-stimulator?			
3.	Do you have a cochlea implant/surgery to your ears? (If yes, please specify)			
4.	Have you ever had heart surgery such as a valve replacement? (If yes, please specify)			
5.	Have you ever had any type of electronic, mechanical, or magnetic implant? (If yes, please specify)			
6.	Do you have any foreign body in your eyes or body? (Bullet fragments etc..)			
7.	Do you have a vena cava filter?			
8.	Do you have a prosthetic limb, eye or other artificial device not already mentioned? (If yes, please specify)			
9.	Are you pregnant or breast feeding?			
10.	Are you claustrophobic?			
11.	Do you have aneurism clips?			
12.	Do you have renal impairment?			
13.	Do you have asthma?			
14.	Do you have allergies? (If yes, please specify)			
15.	Do you have any other implants? (e.g. screws, plates, joint replacements)			
18.	Other			

I hereby acknowledge that the potential risks of the examination have been explained to me and that during the course of the investigation I will receive an intravenous injection of contrast agent.
Attention: It is the policy of this institution not to discuss results of the MR Investigation with the patients for ethical reasons. All enquiries in this regard should be directed to the referring physician.

Participant Signature: _____ **Date:** _____
Consent taken by: _____
Please remove all loose metallic objects, including metallic body piercings, hearing aids and dentures.